(2)

Semiannual Report

Low Temperature Deposition and Characterization of N- and P-Type Silicon Carbide Thin Films and Associated Ohmic and Schottky Contacts

Supported under Grant #N00014-92-J-1500
Office of the Chief of Naval Research
Report for the period April 1, 1992–June 30, 1992

R. F. Davis and R. J. Nemanich*
P. Grigg, R. S. Kern, Y. K. Kim, L. Rowland,
L. Spellman, S. Tanaka and Y. C. Wang
Materials Science and Engineering Department
*Department of Physics
North Carolina State University
Raleigh, NC 27695

June 1992

92

REPORT DOCUMENTATION PAGE

Form Approved
OMB No 0704 0188

1. AGENCY USE ONLY (Leave blank)	2. REPORT DATE	3. REPORT TYPE AND DATES COVERED
	June, 1992	Semiannual April 1, 1992–June 30, 1992

4. TITLE AND SUBTITLE
Low Temperature Deposition and Characterization of N- and P-Type Silicon Carbide Thin Films and Associated Ohmic and Schottky Contacts

5. FUNDING NUMBERS
R&T: sic0002---01
1261
N00179
N66005
4B855

6. AUTHOR(S)
Robert F. Davis

7. PERFORMING ORGANIZATION NAME(S) AND ADDRESS(ES)
North Carolina State University
Hillsborough Street
Raleigh, NC 27695

8. PERFORMING ORGANIZATION REPORT NUMBER
#N00014-92-J-1500

9. SPONSORING/MONITORING AGENCY NAME(S) AND ADDRESS(ES)
Sponsoring: ONR, 800 N. Quincy, Arlington, VA 22217
Monitoring: Office of Naval Research Resider, N66005
The Ohio State Univ. Research Center
1314 Kinnear Road
Columbus, OH 43212-1194

10. SPONSORING/MONITORING AGENCY REPORT NUMBER

11. SUPPLEMENTARY NOTES

12a. DISTRIBUTION/AVAILABILITY STATEMENT
Approved for Public Release—Distribution Unlimited

12b. DISTRIBUTION CODE

13. ABSTRACT (Maximum 200 words)

Gas-source MBE growth of epitaxial layers of 3C (beta)-SiC (111) on Si faces of 6H-SiC {0001} cut 3°–4° towards [11$\bar{2}$0] has been achieved at 1000-1250°C using C_2H_4 and Si_2H_6. The occurrence of 3C-SiC is attributed mainly to the lower surface mobility of the adsorbed species at the temperatures used in this research. Plan-view TEM and RHEED analysis showed a double positioning structure. This combination of high flow (total flow 2.5 sccm) and low temperatures (1050°C) resulted in a very high nucleation density which likely allowed interaction between nuclei very early in growth, leading to a smooth growth surface. Solid solutions and multilayers of AlN and SiC have been grown on 6H-SiC (0001) substrates cut 3°–4° off-axis to [1$\bar{1}$$\bar{2}$0]. Evidence is presented which suggests that the AlN-rich solid solutions are cubic. Multilayer structures of 6H-SiC, 2H-AlN, and 3C-SiC were also fabricated. Finally, studies to understand what controls contact electrical characteristics of specific metals to n-type 6H-SiC has continued in order to select the best ohmic and rectifying contacts. Current-voltage measurements have shown that Ti, Pt, and Hf contacts deposited at room temperature on n-type, (0001) 6H-SiC are rectifying, all with ideality factors between 1.01 and 1.09. The lowest leakage currents (~5×10^{-8} A/cm^2 at –10 V) were found for unannealed Pt contacts and for Hf contacts annealed at 700° for 20 minutes. Current-voltage (I-V), capacitance-voltage (C-V), and x-ray photoelectron spectroscopy (XPS) were among the techniques used to determine barrier heights, all of which were within a few tenths of 1.0 eV. The narrow range of calculated barrier heights along with the XPS valence spectrum of the "clean" SiC surface suggests that the Fermi level is pinned at the semiconductor surface.

14. SUBJECT TERMS	15. NUMBER OF PAGES
silicon carbide, molecular beam epitaxy, solid solutions, aluminum nitride, Schottky contacts, ohmic contacts, leakage current, ideality factor	46
	16. PRICE CODE

17. SECURITY CLASSIFICATION OF REPORT	18. SECURITY CLASSIFICATION OF THIS PAGE	19. SECURITY CLASSIFICATION OF ABSTRACT	20. LIMITATION OF ABSTRACT
UNCLAS	UNCLAS	UNCLAS	SAR

Table of Contents

I. Introduction

Silicon carbide (SiC) is a wide bandgap material that exhibits polytypism, a one-dimensional polymorphism arising from the various possible stacking sequences of the silicon and carbon layers. The lone cubic polytype, β-SiC, crystallizes in the zincblende structure and is commonly referred to as 3C-SiC. In addition, there are also approximately 250 other rhombohedral and hexagonal polytypes [1] that are all classed under the heading of α-SiC. The most common of the α-SiC polytypes is 6H-SiC, where the 6 refers to the number of Si/C bilayers along the closest packed direction in the unit cell and the H indicates that the crystal structure is hexagonal.

Beta (3C)-SiC is finding considerable use in applications that utilize its attractive physical and electronic properties such as wide bandgap (2.2 eV at 300K) [2], high breakdown electric field (2.5×10^6 V/cm) [3], high thermal conductivity (3.9 W/cm °C) [4], high melting point (3103K at 30 atm) [5], high saturated drift velocity (2×10^7 m/s) [6], and small dielectric constant (9.7) [7]. Primarily due to its higher electron mobility than that of the hexagonal polytypes, such as 6H-SiC [8], β-SiC is preferable to hexagonal SiC for most device applications.

Most 3C-SiC thin film growth to date has been performed on Si substrates. Large-area, crack-free, and relatively thick (up to 30 μm) epitaxial 3C-SiC thin films have been grown on Si (100) by exposing the Si substrate to a C-bearing gaseous species prior to further SiC growth [7, 9, 10]. However, these films exhibited large numbers of line and planar defects due to large lattice and thermal mismatches between SiC and Si. One particular type of planar defect, the inversion domain boundary (IDB), was eliminated with the use of Si (100) substrates cut 2°–4° toward [011] [11-13]. Growth on Si substrates has allowed much understanding of SiC growth processes and device development to occur, but the large thermal and lattice mismatches between SiC and Si hamper further development using Si substrates. As a result, great effort has been made to develop methods for growth SiC single crystal substrates for homoepitaxial growth of SiC thin films.

Since the 1950's, monocrystalline single crystals of 6H-SiC have been grown at using the Lely sublimation process [14]. However, nucleation was uncontrolled using this process and control of resultant polytypes was difficult. SiC single crystals inadvertently formed during the industrial Acheson process have also been used as substrates for SiC growth. However, neither these crystals or those formed using the Lely process are large enough for practical device applications. Recently, using a seeded sublimation-growth process, boules of single polytype 6H-SiC of > 1 inch diameter of much higher quality of that obtained using the Lely process have been grown. The use of single crystals of the 6H polytype cut from these boules has given a significant boost to SiC device development.

SiC epitaxial thin film growth on hexagonal SiC substrates has been reported since the 1960's. The use of nominally on-axis SiC substrates has usually resulted in growth of 3C-SiC films. Films of 3C-SiC (111) grown by CVD have been formed on 6H-SiC substrates less than 1° off (0001) [15]. Films of 3C-SiC on 6H-SiC substrates have typically had much lower defect densities than those grown on Si substrates. The major defects present in 3C-SiC/6H-SiC films have been double positioning boundaries (DPB) [16]. Despite the presence of DPBs, the resultant material was of sufficient quality to further device development of SiC. The use of off-axis 6H-SiC (0001) substrates has resulted in growth of high-quality monocrystalline 6H-SiC layers with very low defect densities [17].

In addition, the use of more advanced deposition techniques, such as molecular beam epitaxy (MBE), has been reported for SiC in order to reduce the growth temperature and from about 1400-1500°C on 6H-SiC substrates. Si and C electron-beam sources have been used to epitaxially deposit SiC on 6H-SiC (0001) at temperatures of 1150°C [18]. Ion-beam deposition of epitaxial 3C-SiC on 6H-SiC has also been obtained at the temperature of 750°C using mass-separated ion beams of $^{30}Si^{+}$ and $^{13}C^{+}$ [19].

Aluminum nitride (AlN) is also of particular interest at this time because of its very large bandgap. It is the only intermediate phase in the Al-N system and normally forms in the wurtzite (2H-AlN) structure. Most current uses of AlN center on its mechanical properties, such as high hardness (9 on Mohs scale), chemical stability, and decomposition temperature of about 2000°C [20]. Properties such as high electrical resistivity (typically $\geq 10^{13}$ Ω-cm), high thermal conductivity (3.2 W/cm K) [21], and low dielectric constant ($\varepsilon \approx 9.0$) make it useful as a potential substrate material for semiconductor devices as well as for heat sinks. The wurtzite form has a bandgap of 6.28 eV [22] and is a direct transition, thus it is of great interest for optoelectronic applications in the ultraviolet region.

Because of the difference in bandgaps (2.28 eV for 3C-SiC and 6.28 eV for 2H-AlN) between the materials, a considerable range of wide bandgap materials, made with these materials, should be possible. Two procedures for bandgap engineering are solid solutions and multilayers. A particularly important factor is that the two materials have a lattice mismatch of less than one percent.

Research in ceramic systems suggests that complete solid solubility of AlN in SiC may exist [23]. Solid solutions of the wurtzite crystal structure should have E_g from 3.33 eV to 6.28 eV at 0 K. Although it has not been measured, the bandgap of cubic AlN has been estimated to be around 5.11 eV at absolute zero and is believed to be indirect [24]. Cubic solid solutions should thus have E_g from 2.28 eV to roughly 5.11 eV at 0 K and would be indirect at all compositions if theory holds true.

Because of their similarity in structure and close lattice and thermal match, AlN-SiC heterostructures are feasible for electronic and optoelectronic devices in the blue and infrared

region. Monocrystalline AlN layers have been formed by CVD on SiC substrates [25] and SiC layers have been formed on AlN substrates formed by AlN sputtering on single crystal W [26]. In addition, theory on electronic structure and bonding at SiC/AlN interfaces [24] exists and critical layer thicknesses for misfit dislocation formation have been calculated for cubic AlN/SiC [27]. Note that AlN (at least in the wurtzite structure) is a direct-gap material and SiC is an indirect gap material. Superlattices of these materials would have a different band structure than either constituent element. The Brillouin zone of a superlattice in the direction normal to the interfaces is reduced in size. This reduction in zone size relative to bulk semiconductors causes the superlattice bands to be "folded into" this new, smaller zone. This folding can cause certain superlattice states to occur at different points in k space than the corresponding bulk material states [28]. This can lead to direct transitions between materials which in the bulk form have indirect transitions. This has been demonstrated in the case of $GaAs_{0.4}P_{0.6}$/GaP and $GaAs_{0.2}P_{0.8}$/GaP superlattices, where both constituents are indirect in the bulk form [29]. Whether this is possible in the case of AlN/SiC is unknown, but very intriguing. It may be possible to obtain direct transitions throughout nearly the entire bandgap range with use of superlattices of AlN and SiC. Use of solid solutions in superlattices introduces additional degrees of freedom. For example, the bandgap can be varied independently of lattice constant with proper choice of layer thickness and composition if superlattices of solid solutions of AlN and SiC were formed.

Due to the potential applications of solid solutions and superlattice structures of these two materials, a MBE/ALE system was commissioned, designed, and constructed for growth of solid solutions and heterostructures of these two materials.

A very important additional goal of this research is to understand what controls the contact electrical characteristics of specific metals to n-type 6H-SiC and to use this information to form good ohmic and Schottky contacts. A list of five metals to be studied, which consists of Ti, Pt, Hf, Co, and Sr, was created at the beginning of this research project. The selection process began by taking the simplest case, an ideal contact which behaves according to Schottky-Mott theory. This theory proposes that when an intimate metal-semiconductor contact is made the Fermi levels align, creating an energy barrier equal to the difference between the workfunction of the metal and the electron affinity of the semiconductor. It is the height of this barrier which determines how the contact will behave; for ohmic contacts it is desirable to have either no barrier or a negative barrier to electron flow, while for a good Schottky contact a large barrier is desired.

Although metals were chosen optimistically, i.e. on the basis that they will form ideal contacts, some evidence exists that the contact properties will be more complicated. J. Pelletier et al. [30] have reported Fermi level pinning in 6H-SiC due to intrinsic surface states, suggesting little dependence of barrier height on the workfunction of the metal. In addition, L.

J. Brillson [31, 32] predicts the pinning rate to be higher for more covalently bonded materials. Other complications may arise if the surface is not chemically pristine. A major part of this project will be devoted to determining whether the contacts behave at all ideally, and if not, whether the Fermi level is pinned by intrinsic or extrinsic effects.

Along with examining the barriers of the pure metal contacts, the chemistry upon annealing will be studied and correlated with the resulting electrical behavior. The electrical behavior will be quantified both macroscopically in terms of current-voltage characteristics and microscopically in terms of barrier height. Identification of the phases formed will present the opportunity to attribute the electrical characteristics to the new phase in contact with silicon carbide.

Within this reporting period, 3C-SiC films were grown on single crystals of nominally on-axis 6H-SiC (0001) as well as 6H-SiC substrates cut 3°-4° off (0001) towards [11$\bar{2}$0]. Crystalline quality of these films were determined using reflection high-energy electron diffraction (RHEED). The dependence of temperature and source gas flow rate ratio on surface morphology and growth rate have been investigated. Surface morphology was examined using scanning electron microscopy (SEM). Defects and interfaces were characterized using high-resolution transmission electron microscopy (HRTEM). From this analysis, reasons are discussed for the formation of 3C-SiC despite the presence of large numbers of surface steps on off-axis substrates. Research concerned with the growth of AlSiNC solid solutions and AlN/SiC heterostructures has also been conducted. In this report, evidence is presented that suggests the formation of cubic solid solutions of AlN and SiC as well as evidence of monocrystalline AlN and SiC heterostructure layers on 6H-SiC (0001) substrates cut 3-4° off-axis toward [11$\bar{2}$0]. Lastly, the results of the investigations concerned with the use of Ti, Pt and Hf metals as rectifying contacts on n-type 6H-SiC are described. Several techniques have been and are being implemented to measure barrier heights. Electrical measurements will be presented, along with some observed trends. The experimental procedures, results, discussion of these results, conclusions and plans for future efforts for each of the topics noted above are presented in the following sections. Each of these sections is self-contained with its own figures, tables and references.

References

1. G. R. Fisher and P. Barnes, Philos. Mag. B **61**, 217 (1990).
2. H. P. Philipp and E. A. Taft, in *Silicon Carbide, A High Temperature Semiconductor*, edited by J. R. O'Connor and J. Smiltens (Pergamon, New York, 1960), p. 371.
3. W. von Muench and I. Pfaffender, J. Appl. Phys. **48**, 4831 (1977).
4. E. A. Bergemeister, W. von Muench, and E. Pettenpaul, J. Appl. Phys. **50**, 5790 (1974).
5. R. I. Skace and G. A. Slack, in *Silicon Carbide, A High Temperature Semiconductor*, edited by J. R. O'Connor and J. Smiltens (Pergamon, New York, 1960), p. 24.

6. W. von Muench and E. Pettenpaul, J. Appl. Phys. **48**, 4823 (1977).
7. S. Nishino, Y. Hazuki, H. Matsunami, and T. Tanaka, J. Electrochem Soc. **127**, 2674 (1980).
8. P. Das and K. Ferry, Solid State Electronics, **19**, 851 (1976).
9. K. Sasaki, E. Sakuma, S. Misawa, S. Yoshida, and S. Gonda, Appl. Phys. Lett. **45**, 72 (1984).
10. P. Liaw and R. F. Davis, J. Electrochem. Soc. **132**, 642 (1985).
11. K. Shibahara, S. Nishino, and H. Matsunami, J. Cryst. Growth **78**, 538 (1986).
12. J. A. Powell, L. G. Matus, M. A. Kuczmarski, C. M. Chorey, T. T. Cheng, and P. Pirouz, Appl. Phys. Lett. 51, 823 (1987).
13. H. S. Kong, Y. C. Wang, J. T. Glass, and R. F. Davis, J. Mater. Res **3**, 521 (1988).
14. J. A. Lely, Ber. Deut. Keram. Ges. **32**, 229 (1955).
15. H. S. Kong, J. T. Glass, and R. F. Davis, Appl. Phys. Lett. **49**, 1074 (1986).
16. H. S. Kong, B. L. Jiang, J. T. Glass, G. A. Rozgonyi, and K. L. More, J. Appl. Phys. **63**, 2645 (1988).
17. H. S. Kong, J. T. Glass, and R. F. Davis, J. Appl. Phys. **64**, 2672 (1988).
18. S. Kaneda, Y. Sakamoto, T. Mihara, and T. Tanaka, J. Cryst. Growth **81**, 536 (1987).
19. S. P. Withrow, K. L. More, R. A. Zuhr, and T. E. Haynes, Vacuum **39**, 1065 (1990).
20. C. F. Cline and J. S. Kahn, J. Electrochem. Soc, **110**, 773 (1963).
21. G. A. Slack, J. Phys. Chem. Solids **34**, 321 (1973).
22. W. M. Yim, E. J. Stofko, P. J. Zanzucci, J. I. Pankove, M. Ettenberg, and S. L. Gilbert, J. Appl. Phys. **44**, 292 (1973).
23. See, for example, R. Ruh and A. Zangvil, J. Am. Ceram. Soc. **65**, 260 (1982).
24. W. R. L. Lambrecht and B. Segall, Phys. Rev. B **43**, 7070 (1991).
25. T. L. Chu, D. W. Ing, and A. J. Norieka, Solid-State Electron. **10**, 1023 (1967).
26. R. F. Rutz and J. J. Cuomo, in *Silicon Carbide-1973*, ed. by R. C. Marshall, J. W. Faust, Jr., and C. E. Ryan, Univ. of South Carolina Press, Columbia, p. 72 (1974).
27. M. E. Sherwin and T. J. Drummond, J. Appl. Phys. **69**, 8423 (1991).
28. G. C. Osbourn, J. Vac. Sci. Technol. B **1**, 379 (1983).
29. P. L. Gourley, R. M. Biefeld, G. C. Osbourn, and I. J. Fritz, *Proceedings of 1982 Int'l Symposium on GaAs and Related Compounds* (Institute of Physics, Berkshire, 1983), p. 248.
30. J. Pelletier, D. Gervais, and C. Pomot, J. Appl. **55**, 994 (1984).
31. L. J. Brillson, Phys. Rev. B, **18**, 2431 (1978).
32. L. J. Brillson, Surf. Sci. Rep., **2**, 123 (1982).

II. Gas-Source Molecular Beam Epitaxy of 3C-SiC on Off-axis 6H-SiC

A. Experimental Procedures

Films were grown on Si faces of 6H-SiC {0001} substrates grown by a modified sublimation method and provided by Cree Research, Inc. The substrates used in this study were of two types: nominally on-axis (± 0.5° of (0001)), and off-axis (3°-4° off (0001) towards [11$\bar{2}$0]). Substrate orientation was measured by X-ray diffraction using the Laue transmission method. Films were grown using a MBE system described in previous reports. Samples were chemically cleaned prior to growth using a 10% HF etch at room temperature for 5 min, followed by a DI water rinse for 2 min. This limited cleaning process has been shown to retard formation of a carbon-rich surface layer on 6H-SiC [1].

In order to further clean the SiC surface, the sample was heated in the growth system at the growth temperature (1000-1250°C) for 5 min prior to growth. Then 3C-SiC was formed by introducing Si_2H_6 and C_2H_4. The flow ratio between Si_2H_6 and C_2H_4 was independently varied from 1:1 to 1:8 at the highest growth temperature (1250°C). The effect of total flow rate for a Si_2H_6 to C_2H_4 ratio of 2:1 was also examined at this temperature. In addition, other experiments were performed to determine the effect of temperature at source flow ratios of 1:2 and 1:4. Pressures during growth were 3×10^{-6}-6×10^{-5} torr, with the system base pressure being less than 1×10^{-9} torr. In order to determine thickness, Al was intentionally introduced into some films by a MBE effusion cell. All films discussed in this study were grown for 210 to 300 min.

Surface morphology of the resultant films was examined using field-emission scanning electron microscopy (SEM). High-resolution transmission electron microscopy (HRTEM) was employed to determine the defects present in the film as well as examining the film/interface region. An Ashaki UHR 002B HRTEM was used for this purpose.

B. Results

1. General

All films obtained in this study were determined by RHEED to be 3C-SiC. Figure 1 (a) shows the RHEED pattern ([110] zone axis) from a film grown at 1250°C on 6H-SiC (0001) cut 3°–4° towards [11$\bar{2}$0] at 0.1 sccm Si_2H_6 and 0.2 sccm C_2H_4. A large number of Kikuchi lines are present which are an indication of the high quality and smoothness of the sample. Extra streaks in the pattern actually result from double positioning boundaries, which result when two adjacent 3C-SiC (111) nuclei form rotated 60° to each other about the <111> axis [16]. These have also been seen in RHEED on converted SiC (111) layers formed on Si (111) [2, 3], though because of the large mismatch between SiC and Si, the double positioning structure consisted of doublets of spots rather than streaks.

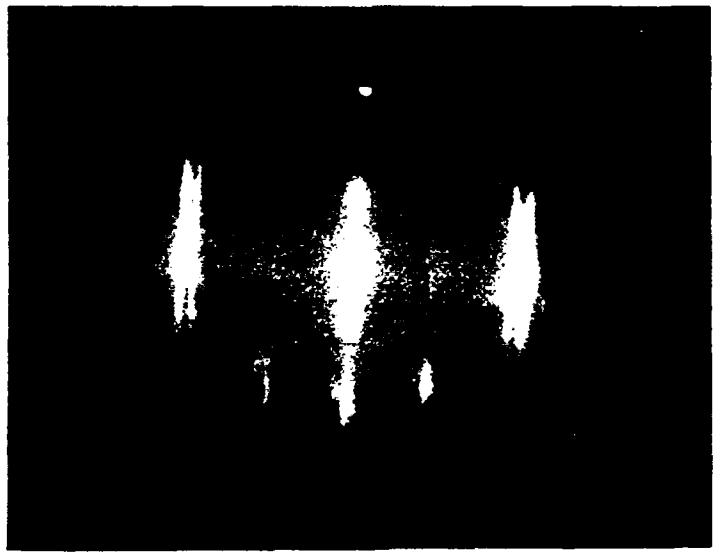

(a)

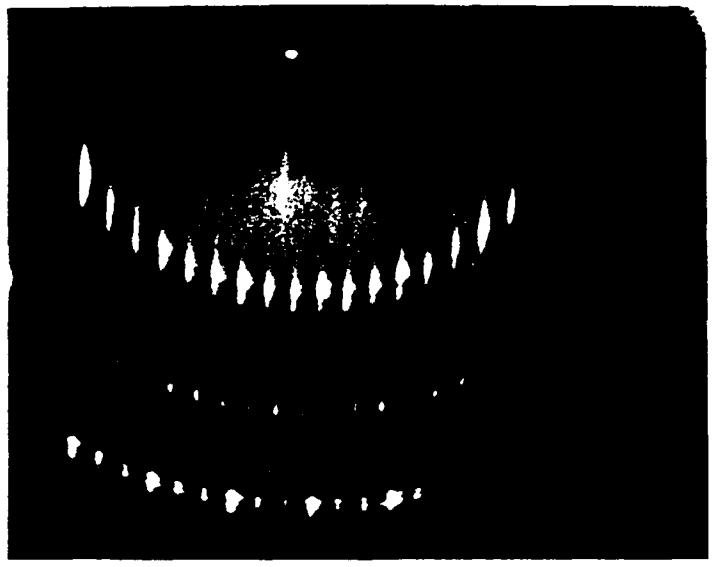

(b)

Figure 1. Reflection high-energy electron diffraction patterns ([110] azimuth) of 3C-SiC films grown at (a) 1250°C, 0.2 sccm C_2H_4 and 0.1 sccm Si_2H_6, and (b) 1000°C, 0.2 sccm C_2H_4 and 0.1 sccm Si_2H_6.

In general streaking in the patterns and the presence of Kikuchi lines made photography and interpretation of [110] RHEED patterns difficult. The difficulty in obtaining and interpreting [110] zone axis RHEED patterns from overlap of Kikuchi lines was likely due to the double positioning structure of the films. Other zone axes also showed a doubling of reflections caused by the double positioning boundaries. Figure 1 (b) is a RHEED pattern of the [211] zone axis reflection from the sample shown in Figure 1 (a). Growth of SiC, however, at 1000°C using 0.2 sccm C_2H_4 and 0.1 sccm Si_2H_6 resulted in a film whose diffraction pattern changed markedly with rotation of the substrate with the respect to the electron beam, but the pattern from the <110> azimuth was not visible. Instead, a pattern with streaked Laue zones was obtained as shown in Figure 1 (c). Evidence of this pattern and detecting differences between this pattern and the hexagonal $<2\bar{1}\bar{1}0>$ azimuth is the most obvious method to determine that a film is cubic by RHEED. The change in pattern with orientation showed the sample was single crystal in nature.

All films appeared smooth to the naked eye and when film and substrate were viewed, but places where growth occurred appeared slightly darker than those shadowed by the sample holder. Higher magnifications, however, showed differences between various film conditions. The surface morphology of films with different source flow ratios was examined at 1250°C. The flow rate for Si_2H_6 was kept constant at 0.50 sccm while the C_2H_4 flow rate was varied from 1.00 to 4.00 sccm, resulting in a 2:1 to 8:1 C:Si source ratio as both Si_2H_6 and C_2H_4 have 2 atoms/molecule of source gas. Figure 2 (a) is a high-magnification SEM micrograph taken of a sample grown with a 2:1 Si_2H_6 to C_2H_4 ratio. This film has a high density of small nuclei (200 to 400 nm wide) which are bounded by sides which are 60° or 120°. However, these nuclei appear smooth on their top surface. Two orientations of nuclei can be seen in the micrograph which are rotated 60° to each other (note arrows for positions of misoriented nuclei). These two orientations of nuclei cause double positioning boundaries upon their coalescence [4]. As the amount of ethylene is increased so that the Si-to-C ratio is 1:8, the film exhibits a mosaic structure as shown in Figure 2 (b). Ledges and wavy lines of darker contrast on the surface have been identified by other researchers as DPBs [5].

As mentioned in the Introduction, 3C-SiC films with a double positioning structure have been obtained by several research groups using CVD. The substrates used for this growth of 3C-SiC on 6H-SiC, however, have been SiC oriented within 1° of (0001). Whenever substrates oriented off (0001) 3-4° towards $[11\bar{2}0]$ have been used as were used in this study, 6H-SiC growth has occurred [6–8]. The only reported occurrence of 3C-SiC in CVD growth on SiC {0001} samples oriented 3°-4° towards $[11\bar{2}0]$ was only in small islands distributed on the 6H-SiC surface when high flow rates of source gases were used at 1350°-1550°C. Growth was performed on the C face in the SiH_4-C_2H_4-H_2 system [9]. This result implies that

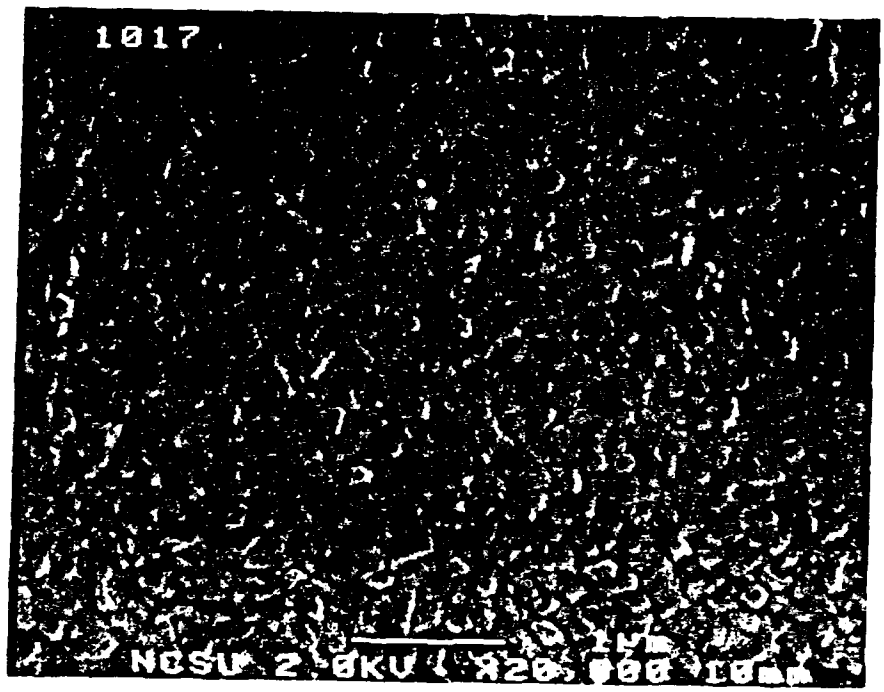

(a)

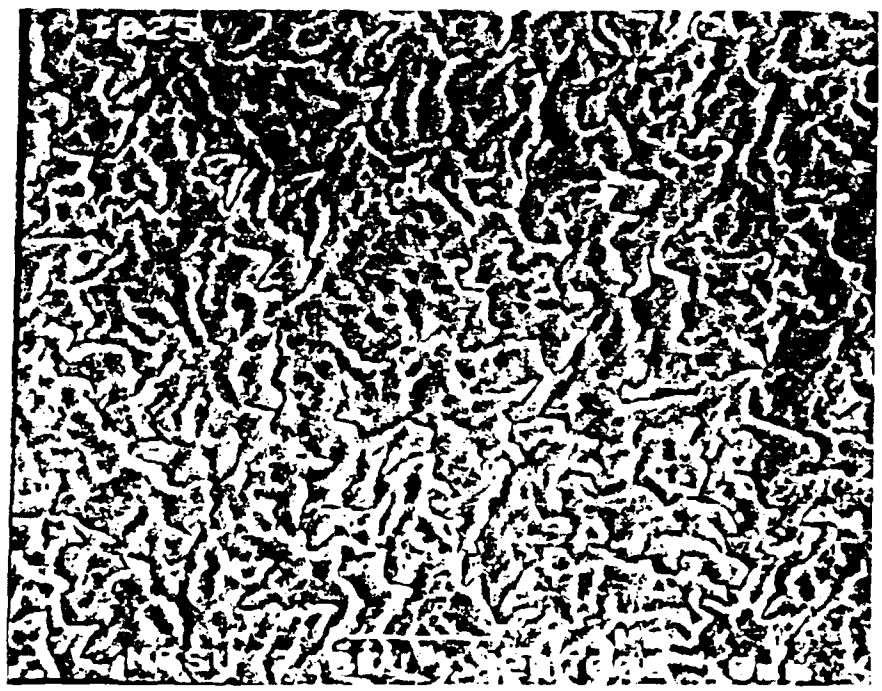

(b)

Figure 2. Scanning electron micrographs of surface of 3C-SiC films grown at 1250°C using (a) 1.0 sccm C_2H_4 and 0.5 sccm Si_2H_6 and (b) 4.0 sccm C_2H_4 and 0.5 sccm Si_2H_6.

increasing supply of SiC source gases may increase the likelihood of obtaining 3C-SiC. If the flux of source gases is decreased, then adsorbed atoms or Si- or C-containing species would have a longer time (on average) to migrate on the growing surface before reacting with other growth species. If a sufficient density of steps are present on the surface and if the mobility of adsorbed species is large enough, adsorbed species should more easily be able to find kinks which can act as incorporation sites for lateral growth. Sufficient nucleation at kinks caused by surface steps should lead to lateral growth of steps and these steps serve as a template for growth. This is believed to be the cause of formation of 6H-SiC on SiC {0001}cut 3°-4° towards [11$\bar{2}$0] [6]. If these steps are not present in sufficient density, there is insufficient surface mobility (i.e., temperature), or species arrive at too high a flux, then atoms will be unable to find steps and will nucleate two-dimensionally on the flat areas between steps. At the relatively low temperatures used in SiC thin-film research, 3C-SiC (111) will form without influence from steps, as growth of SiC on nominally on-axis SiC substrates usually results in 3C-SiC. As a result, the effect of temperature and flow rate reduction on step nucleation and formation of 6H-SiC was examined in the following section.

2. Effect of Flow Rate

The surface morphology of samples grown at 1250°C with different flow rates (Si:C source flow ratio kept at 2:1) is shown in Figure 3. A total flow rate of 3.0 sccm resulted in a very rough surface, as shown in Figure 3 (a). This surface is covered with a very high density of small (0.1–0.2 μm) nuclei due to the large amount of reactive species available to the SiC substrate. The abundance of reactive species due to the large flow rate also caused vertical growth of these nuclei to dominate over lateral growth and coalescence of these nuclei did not occur. A total flow rate of 1.5 sccm (as in Figure 2 (b)) produced a somewhat smoother surface. Vertical growth still dominated over lateral growth, though some coalescence of nuclei did occur.

A much lower total flow rate of 0.30 sccm (Figure 3 (b)), however, resulted in a smoother film with fewer, smaller nuclei. The nuclei are more widely spaced and lateral growth is allowed to occur. Growth at 1250°C using a total flow rate of 0.06 sccm was also attempted, but no film was detected by HRTEM analysis. However, even in the case of low flow, all films were 3C-SiC (111).

Figure 4 is a cross-sectional HRTEM micrograph of part of the film and the 3C-SiC/6H-SiC interface. The substrate is oriented so that the [11$\bar{2}$0] direction of the 6H-SiC substrate is perpendicular to the plane of the image. From the lattice images of the film, the grown layer is deduced to be cubic and in the (111) orientation. The epitaxial relationship between the

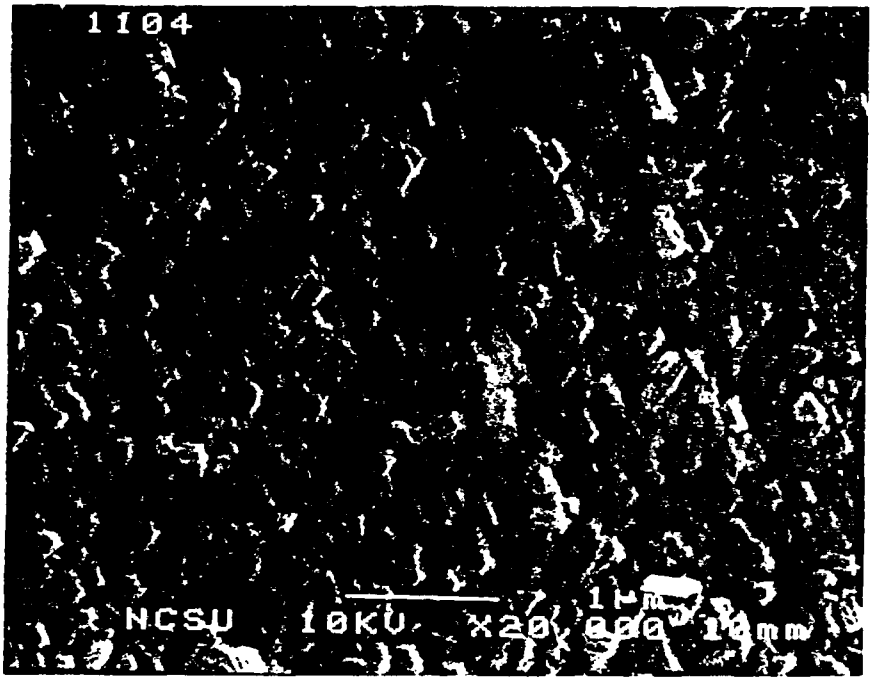

(a)

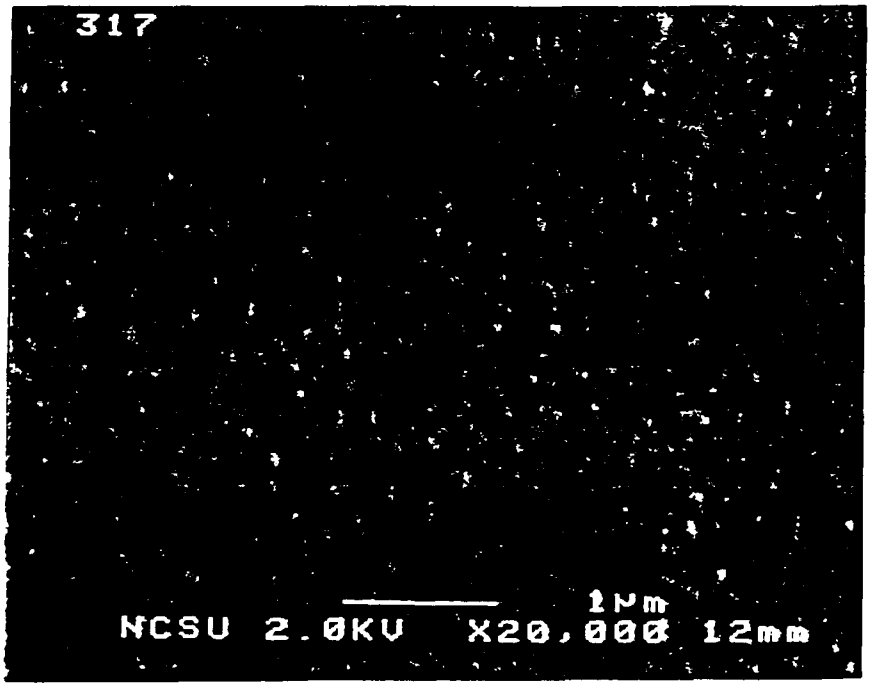

(b)

Figure 3. Scanning electron micrographs of surface of 3C-SiC films grown at 1250°C using (a) 2.0 sccm C_2H_4 and 1.0 sccm Si_2H_6 and (b) 0.2 sccm C_2H_4 and 0.1 sccm Si_2H_6.

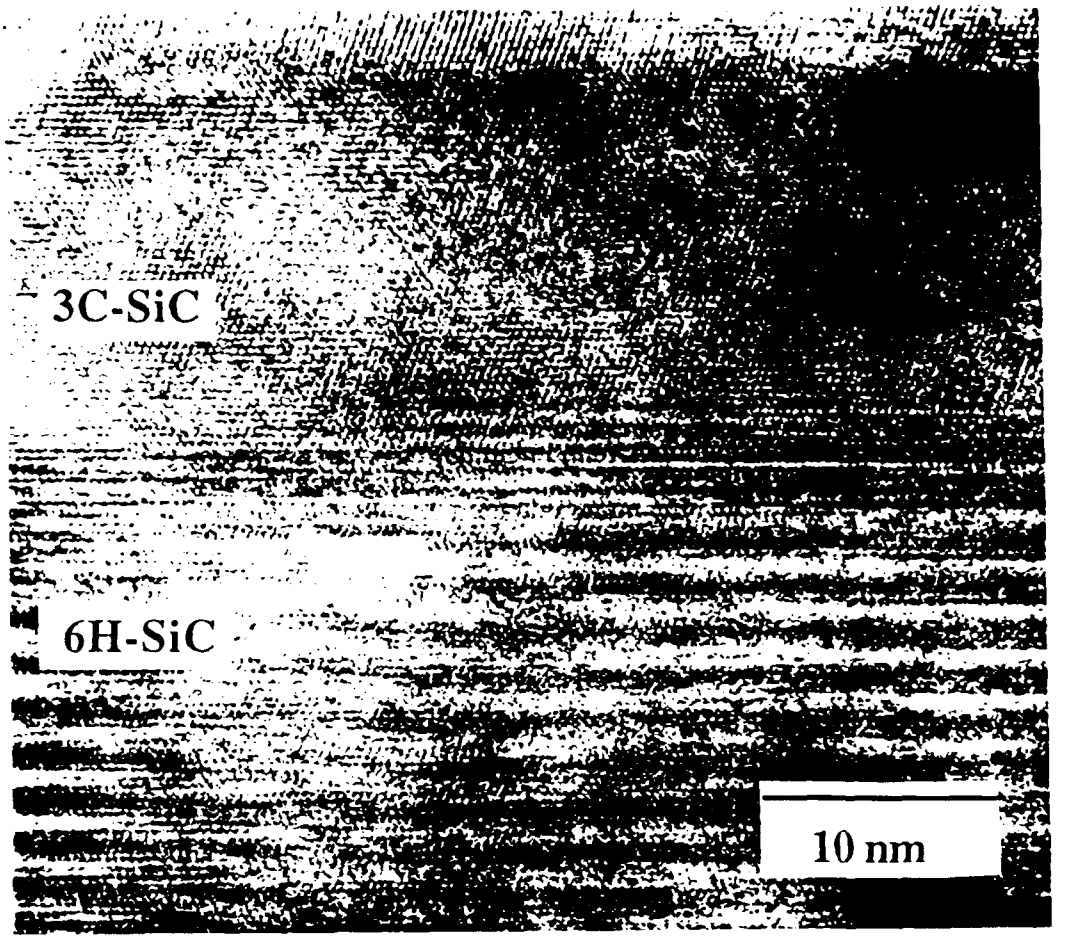

Figure 4. Cross-sectional high resolution transmission electron micrograph of 3C-SiC (111) film on off-axis 6H-SiC (0001) substrate. Steps on the substrate surface can be seen. Sample was grown at 1200°C using 1.0 sccm C_2H_4 and 0.5 sccm Si_2H_6.

substrate and the 3C-SiC film can be seen from the high-resolution micrograph and the corresponding SAD pattern. Plan-view TEM on this sample (Figure 5) shows that DPBs and stacking faults (denoted SF) are present on this sample.

Steps on the 6H-SiC are readily visible in Figure 4, but their height is several atoms high, rather than biatomic steps, which would be expected. This is strong evidence that significant step bunching is occurring on the 6H-SiC surface prior to growth. Lower temperatures in the thermal desorption step might serve to limit step bunching and enable 6H-SiC to form on the growing surface. Also, lower temperatures will decrease mobility of adsorbed species on the surface and limit the ability of Si- and C-containing species to locate steps, which would likely result in 6H-SiC. Given these tow competing factors for nucleation on steps (step migration and bunching, and surface mobility), the temperature was varied to observe the effect of T on resultant polytype and morphology.

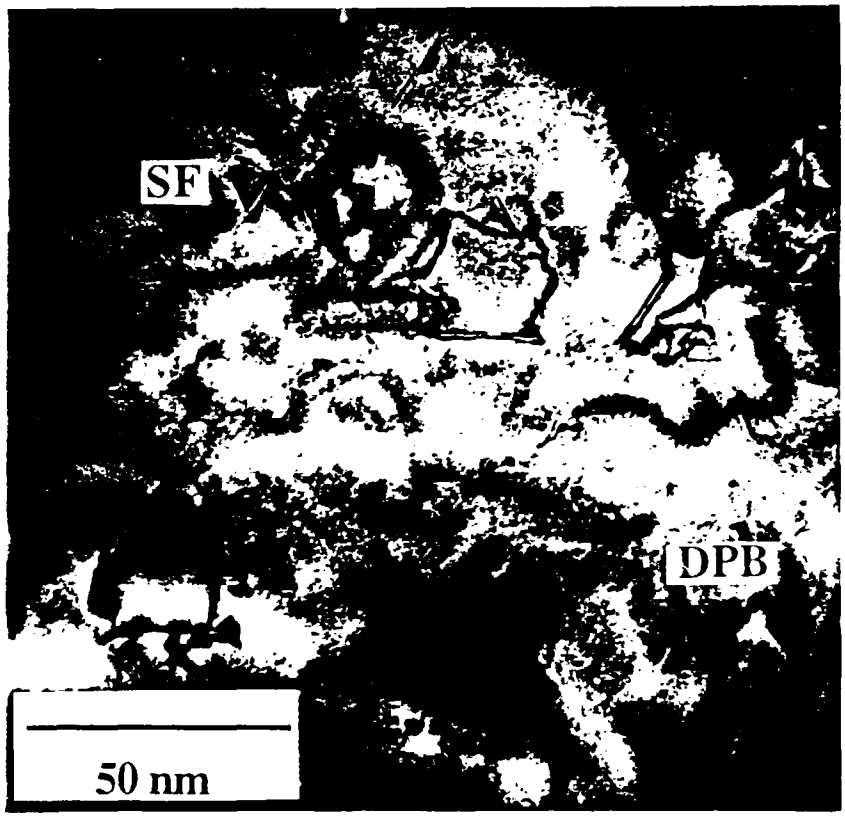

Figure 5. Plan-view transmission electron micrograph of 3C-SiC film and 6H-SiC substrate. Both stacking faults (denoted SF) and double positioning boundaries are visible in the micrograph.

3. Effect of Temperature

The growth temperature was varied in the range 1000-1250°C in order to observe the effect of temperature on resultant morphology and polytype. Because of the improvement in morphology at lower flow rates, and because lower flow rates will decrease nucleation density, lower flow rates were used. Figure 6 shows a SEM micrograph of films grown on an off-axis 6H-SiC (0001) substrate using 0.20 sccm C_2H_4 and 0.10 sccm Si_2H_6 at (a) 1200°C and (b) 1000°C. The morphology in these can be compared to that obtained at 1250°C (Figure 2 (c)). The film morphology at 1200°C is similar to that obtained at 1250°C, but nuclei are more closely spaced. The decrease in temperature should cause an increase in nucleation density as surface species will not have mobility to travel large distances on the substrate surface. As a result, Si- and C-containing species will cluster in nuclei which are more closely spaced. Oddly, the surface roughness decreases at 1000°C, but as seen in Figure 6 (b), widely spaced faceted surface features of 0.2-0.5 μm occur throughout the film. Otherwise, the film appears smooth even at high magnification and the effect of large numbers of small nuclei cannot be seen. As with the case of lower flow rates, all films obtained at lower temperatures were 3C-SiC.

The film at 1000°C (Figure 6 (b)) should have a higher nucleation density than film grown under the same conditions at 1200°C, but appears smoother at high magnification. One possible explanation is the nucleation density on the substrate is sufficiently high for these individual nuclei to interact upon their formation. As nuclei become more closely spaced, their interaction should increase. If the interaction between nuclei increased, it is conceivable that misoriented nuclei (due to double positioning) could reorient themselves and DPBs could be eliminated. Also, this interaction between nuclei should also smoothen the film, as they would coalesce after reaching only a small number of atoms in size.

In order to examine the possibility of improvement of film quality by increasing nucleation density, a film was grown at low temperature (1050°C) and high flow rate (0.50 sccm Si_2H_6 and 2.00 sccm C_2H_4). The RHEED pattern ([110] azimuth) for this film is shown in Figure 7 (a). The extremely high degree of streaking is indicative of a very smooth film. A SEM micrograph of the surface at 20,000x is shown in Figure 7 (b). The film appears much smoother than those at higher temperature and those at lower flow rates. These growth conditions were the best found in this study. However, the double positioning structure was still observed in the RHEED pattern.

C. Discussion

The effect of surface steps, which is so important in CVD growth, appears not to have an effect in MBE growth at 1250°C, at least with the step density obtained with a 3° to 4° misorientation. The similarity in film morphology and resultant SiC polytype between on- and off-axis SiC (0001) suggests that the orientation difference between the substrates does not affect nucleation and growth processes in MBE growth of SiC under the conditions used in this study. The effect of surface steps, though very important in CVD growth on 6H-SiC (0001) substrates cut 3°-4° towards [11$\bar{2}$0], plays no obvious role in the gas-source MBE growth presented herein. Even though the step density is high on these off-axis samples, it is apparently not high enough for sufficient nucleation to occur to cause the steps to serve as a template for 6H-SiC growth. Increasing the angle of substrate orientation towards [11$\bar{2}$0] may increase step density enough to induce nucleation along steps and obtain 6H-SiC films. Due to a lack of substrate availability, the effect of step density was not examined.

Several researchers [5, 6, 10] have suggested that variations in surface treatment prior to growth can change the density of or virtually eliminate DPBs formed on the resultant film. Cleaning and pre-growth treatment has also affected formation of 3C-SiC over 6H-SiC on wafers oriented within 1° of {0001} [10], but for wafers oriented several degrees towards [11$\bar{2}$0], cubic SiC has never been formed, no matter what the surface condition. As this growth was done in a ultra-high vacuum environment, the surface condition after a thermal desorption

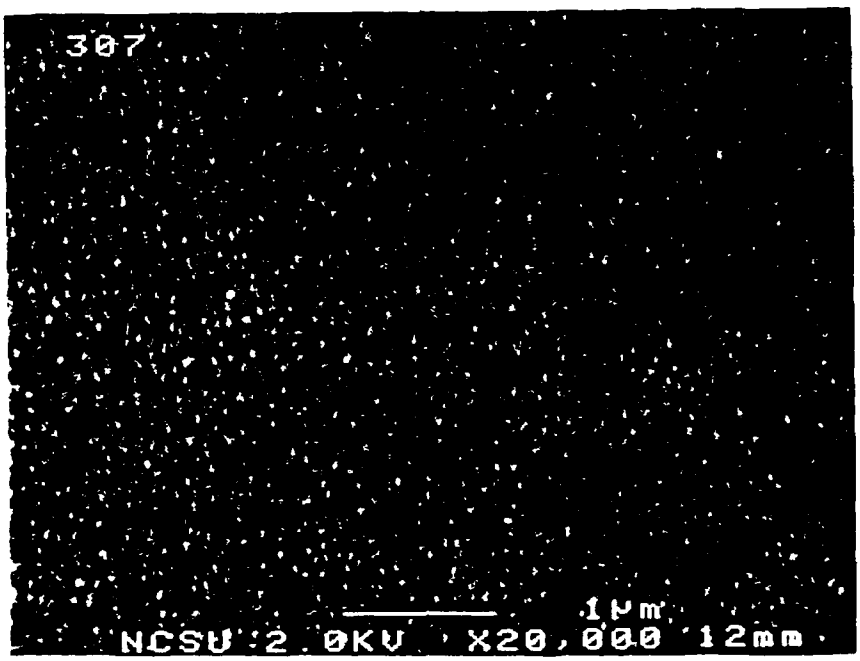

(a)

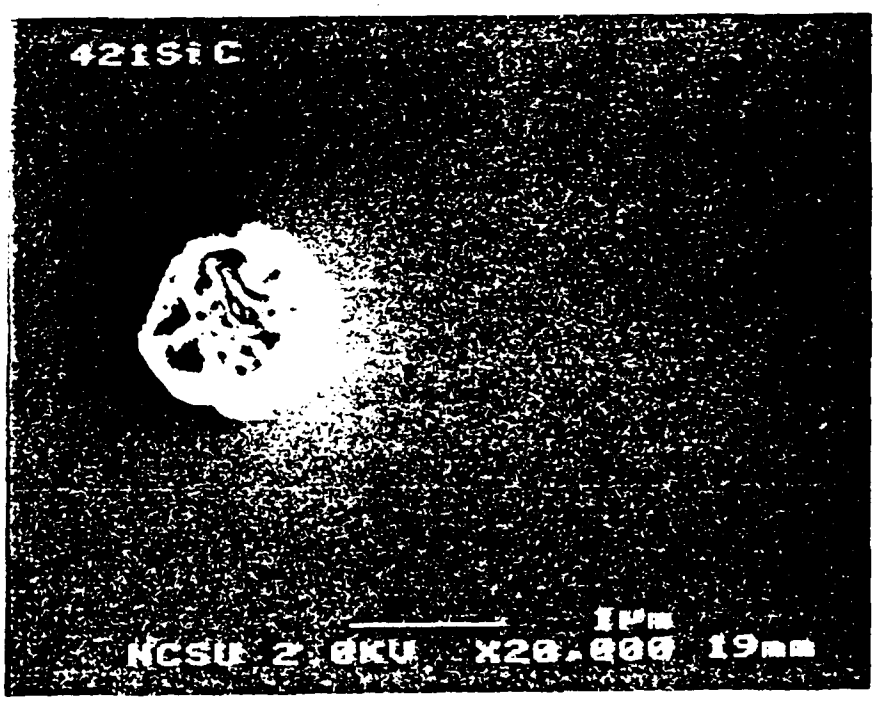

(b)

Figure 6. Scanning electron micrographs of surface of 3C-SiC films grown at low flow rates using 0.2 sccm C_2H_4 and 0.1 sccm Si_2H_6 at (a) 1200°C and (b) 1000°C

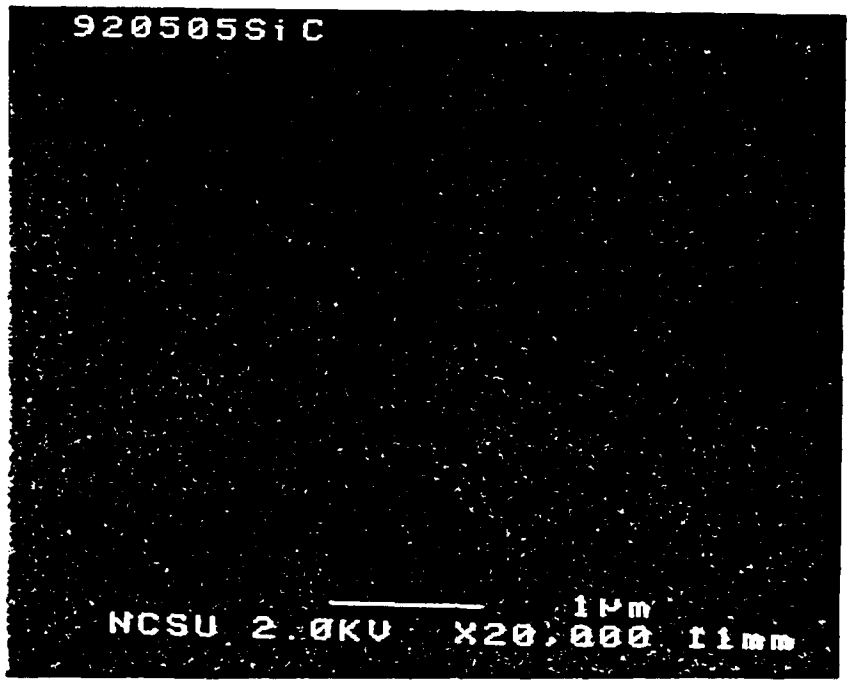

(a) Scanning electron micrograph

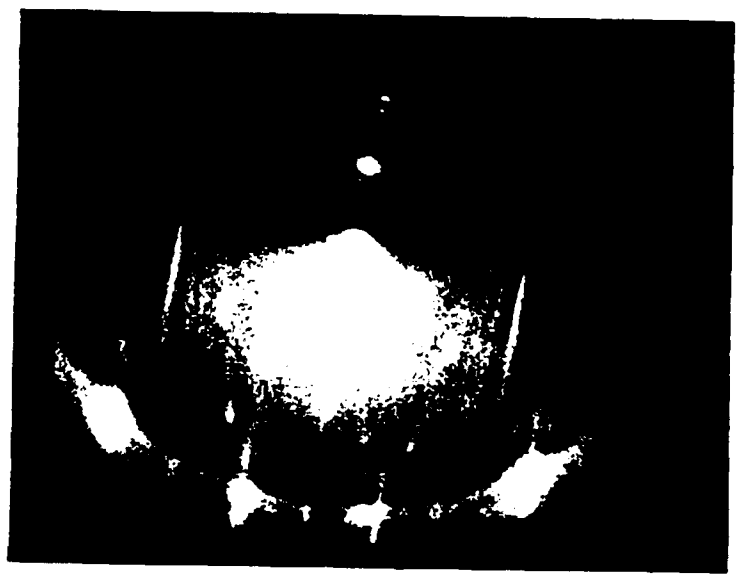

(b) RHEED pattern of [110] azimuth

Figure 7. (a) Scanning electron micrograph of surface and (b) RHEED pattern of 3C-SiC film grown at 1050°C using 2.0 sccm C_2H_4 and 0.5 sccm Si_2H_6.

step should have been better than that obtained after a H_2 or HCl etch step for CVD-grown material. Thus it is unlikely that impurity nucleation is the sole reason for 3C-SiC formation.

In general, both in thin-film and bulk growth, the 3C polytype is usually obtained at lower temperatures than the 6H polytype, and there are many instances where growth below a certain temperature gives 3C-SiC and a higher temperature for growth results in 6H-SiC or other hexagonal polytypes. Campbell and Chu [11] grew SiC using $SiCl_4$ and CCl_4 on natural 6H-SiC (0001) substrates and observed that below 1750°C, cubic layers were formed, while above 1750°C, hexagonal layers were formed. Jennings et al. [12] reported epitaxial growth of SiC on the natural {0001} planes of 6H-SiC substrates using the $SiCl_4$-CCl_4-H_2 system from 1550-1775°C. A mainly cubic layer was obtained which had a mosaic morphology, which is now known to be due to double positioning. At greater than 1725°C, they obtained an epitaxial 6H-SiC if the layer was grown on a mechanically polished substrate. Yoshida et al. [13] obtained epitaxial 3C-SiC (111) on natural (on-axis) Si faces of SiC (0001) by CVD in the temperature range 1350°-1500°C, while at 1700-1800°C they obtained 6H-SiC (0001). Based on these observations by other researchers, at temperatures higher than those used in this study, MBE growth on off-axis substrates may result in growth of 6H-SiC. It is extremely difficult, however, to heat to such high temperatures in a ultra-high vacuum environment. The feasible temperature limit for heating using this MBE system is about 1250°C. As a result, higher temperatures are unlikely to be studied here. Lower temperatures would reduce the driving force for step bunching and might allow for more nucleation on steps, but these lower temperatures also reduced surface mobility. Thus, 3C-SiC was obtained.

However, the best quality film was obtained using high flow and low temperatures. This implies several things. First, because the films at lower temperatures were smoother under these conditions, it could be assumed that conditions are approaching layer-by-layer growth. However, classical nucleation theory states that the arrival rate of species should be low and surface diffusion high in order to obtain layer-by-layer growth. These two statements are inconsistent, so true layer-by-layer growth was not achieved.

Second, films grown in this study have a very low growth rate (10-50 nm/hr). The primary hindrance for growth is likely the reaction of ethylene with disilane. Ethylene will likely not react appreciably with SiC at 1050°C, but with disilane present, which decomposes at much lower temperatures and readily reacts with ethylene, SiC should easily form. If the supply of both reactant species was greatly increased, then more nuclei should form. Also, these nuclei would reach critical size more quickly. If these nuclei were very closely spaced, then these very small three-dimensional clusters would have to interact before becoming too large and might coalesce after reaching only a few atomic distances in thickness.

Another possibility is that at higher temperatures, many of the adsorbed species do not reside on the surface long enough to react and desorb. The vapor pressure of Si at the highest

growth temperatures used (1250°C) is about 10^{-5} torr, which is the same order of magnitude as the pressure of disilane in the system during growth. Therefore, the free Si leaving the surface is barely replaced by the disilane reaching the surface and this may impede growth. Unlike the case of CVD, there is no overpressure of carrier gas to collide with desorbed species and cause many of them to re-adsorb. Once an Si atom or Si-containing molecule desorbs from the nucleating film in a MBE environment, it will likely not collide with other molecules and has essentially a zero chance of returning.

If the flow is very small, then all of the Si may desorb before reaction and SiC will not form. In fact, SiC did not form at extremely low flow rates at 1250°C and a short experiment performed at 1350°C. The Si species may reside longer on places with higher surface energy, such as impurity sites or defects. Thus the supply of free Si to react with C_2H_4 may be limited to impurity sites at combinations of low flow rates and high temperatures and film quality is relatively poor. If the temperature is decreased or flux of source gases is increased, there will be a greater supply of Si and nucleation sites will not be limited to higher-energy sites. As a result, SiC can nucleate throughout the film and the film is of improved quality.

D. Conclusions

Gas-source MBE growth of epitaxial layers of 3C-SiC (111) on 6H-SiC (0001) cut 3°-4° towards [11$\bar{2}$0] has been achieved at 1000-1250°C using C_2H_4 and Si_2H_6 as source gases. This growth temperature is much lower than that typically used in CVD, but previous growth on substrates of the orientation used herein has always resulted in 6H-SiC. High-resolution TEM of a representative film demonstrated the epitaxial relationship between film and substrate. Plan-view TEM and RHEED analysis showed a double positioning structure due to the existence of two equivalent nucleation sites for (111) material on a (111) or (0001) surface as well as stacking faults.

As a result, growth conditions were altered in order to see the effects of changing step mobility (by decreasing temperature) and reducing nucleation density (by reducing flow). Improvements in morphology were obtained but no changes in polytype were obtained with changes in temperature and flow rates of source gases. The occurrence of 3C-SiC (despite the presence of large numbers of surface steps) is attributed mainly to the lower surface mobility of adsorbed species at the temperatures used in this research. Growth using high flow (total flow 2.5 sccm) and low temperatures (1050°C) resulted in a smooth morphology. This combination of high flow and low temperatures resulted in a very high nucleation density which likely allowed interaction between nuclei very early in growth, leading to a smooth growth surface.

E. Future Work

Attempts will be made to obtain lower-temperature growth of SiC using an electron cyclotron resonance (ECR) plasma for downstream decomposition of CH_4. Methane will be used because a single carbon atom is contained in each molecule and no double or triple carbon bonds will need to be broken at the growth surface. In addition, attempts will be made to determine conditions which form 3C-SiC without DPBs and 6H-SiC films on off-axis substrates.

Electrical measurements have proved difficult due to the low growth rates and roughness of the films. Aluminum was successfully incorporated into several of these films (see for example the previous report), but as yet, these films appear to be more conductive than expected using four-point probe measurements. A Hall measurement system was recently constructed in our laboratory and more complete electrical measurements on these films will soon be performed.

F. References

1. L. M. Spellman, private communication.
2. I. H. Khan and R. N. Summergrad, Appl. Phys. Lett. 11, 12 (1967).
3. A. S. Brown and B. E. Watts, J. Appl. Cryst. 3, 172 (1970).
4. M. H. Jacobs and M. J. Stowell, Phil. Mag. 11, 591 (1965).
5. H. S. Kong, J. T. Glass and R. F. Davis, J. Appl. Phys. **64**, 2672 (1988).
6. S. Kaneda, Y. Sakamoto, T. mihara, T. Tanaka, J. Cryst. Growth **81**, 536 (1987).
7. H. Matsunami, K. Shibahara, N. Kuroda, and S. Nishino, in *Amorphous and Crystalline Silicon Carbide*, Springer Proc. in Physics, v. 34, edited by G. L. Harris and C. Y.-W. Wang (Springer-Verlag, Berlin, 1989), pp. 34-39.
8. J. A. Powell, D. J. Larkin, L. G. Matus, W. J. Choyke, J. L. Bradshaw, L. Henderson, M. Yoganathan, J. Yang, and P. Pirouz, Appl. Phys. Lett. 56, 1353 (1990).
9. Y. C. Wang and R. F. Davis, J. Electron. Mater. 20, 869 (1991).
10. S. P. Withrow, K. L. More, R. A. Zuhr and T. E. Haynes, Vacuum **39**, 1065 (1990).
11. R. B. Campbell and T. L. Chu, J. Electrochem. Soc. 113, 825 (1966).
12. V. J. Jennings, A. Sommer, and H. C. Chang, J. Electrochem. Soc. 113, 728 (1966).
13. S. Yoshida, E. Sakuma, H. Okumura, S. Misawa, and K. Endo, J. Appl. Phys. 62, 303 (1987).

III. AlN/SiC Solid Solutions and Layered Heterostructures

A. Experimental Procedure

These films were grown on Si faces of 6H-SiC (0001) substrates provided by Cree Research, Inc. The substrates used in this study were found to be off-axis (3-4° off (0001) toward [11$\bar{2}$0]) by X-ray diffraction using the Laue back-reflection method. Films were grown using the MBE system detailed in previous reports, and readers are referred to these reports for a description and schematic of the system. Sources used are as follows: disilane (Si_2H_6) for silicon, ethylene (C_2H_4) for carbon, gaseous nitrogen (N_2) introduced through an ASTeX Compact ECR electron cyclotron resonance (ECR) plasma source for nitrogen, and an MBE effusion cell for evaporation of solid aluminum. Samples were chemically cleaned prior to growth in a 10% HF solution for 5 min, followed by a DI water rinse for 2 min. All of the experiments were done in excess of 1000°C, thereby desorbing any hydrocarbons or oxide layers from the SiC surface.

1. Solid Solution Procedure

Solid solutions of SiC and AlN were formed by GSMBE on the 6H-SiC substrates using the following conditions: Si_2H_6 flow, 0.1 sccm; C_2H_4 flow, 0.2 sccm; N_2 flow "diluted" with argon (about a 10:1 Ar to N_2 ratio) to an operating pressure of 1.6×10^{-4} torr; Al source temperature, 1050°C; sample temperature, 1050°C; and time, 240 minutes. Pressures during growth typically reached 2×10^{-4} torr, with the system base pressure being less than 1×10^{-9} torr.

Reflection high-energy electron diffraction (RHEED) was used to determine the crystalline quality of the surface of the resultant films. In addition, the chemical composition and depth profile of each sample were obtained using a scanning Auger microprobe. Because the films were very thin (<100 Å) and polycrystalline, no further analysis was performed.

2. Multilayer Procedure

Superlattices, or multilayers, of SiC and AlN were formed by GSMBE on the 6H-SiC substrates using the following conditions. First, the AlN layers were grown using the following conditions: Al source temperature, 1210°C; N_2 flow to an operating pressure of 1.6×10^{-4} torr; and time, 20 minutes. Next, the SiC layers were grown using the following conditions: Si_2H_6 flow, 0.1 sccm; C_2H_4 flow, 0.2 sccm and time, 150 minutes. The entire growth run was performed with a sample temperature of either 1050°C or 1200°C. Pressures during growth typically reached 2×10^{-4} torr, with the system base pressure being less than 1×10^{-9} torr.

Reflection high-energy electron diffraction (RHEED) was used to determine the crystalline quality of the surface of the resultant films. Those films that were monocrystalline by RHEED

were further analyzed. The chemical composition and depth profile of each sample were obtained using a scanning Auger microprobe. A field-emission scanning electron microscope (SEM) was used to observe surface morphology. And, high-resolution transmission electron microscopy (HRTEM) was employed to determine the defects and crystalline structure present in the film as well as examining the film/interface region. An Ashaki EM-002B HRTEM was used for this purpose.

B. Results

1. Solid Solutions

Figure 1 shows a RHEED photograph of an AlN-SiC sample grown under the procedure described above. Note that the pattern consists of both spots and rings. The spots correspond to a [110] zone axis in the cubic system. The rings, which are invariant with respect to orientation, indicate that the film is polycrystalline.

Figure 1: RHEED image of an AlN-SiC solid solution on a 6H-SiC substrate taken after growth.

An Auger depth profile of the AlN-SiC film is shown in Figure 2. As the graph indicates, the film is about 72% AlN and 28% SiC. It is also important to note that the amount of carbon in the film is lower throughout the film despite being added in a 2:1 ratio to silicon. Also, since the sputtering rate was approximately 90 Å/min, the thickness of this film can be roughly estimated as about 80 Å.

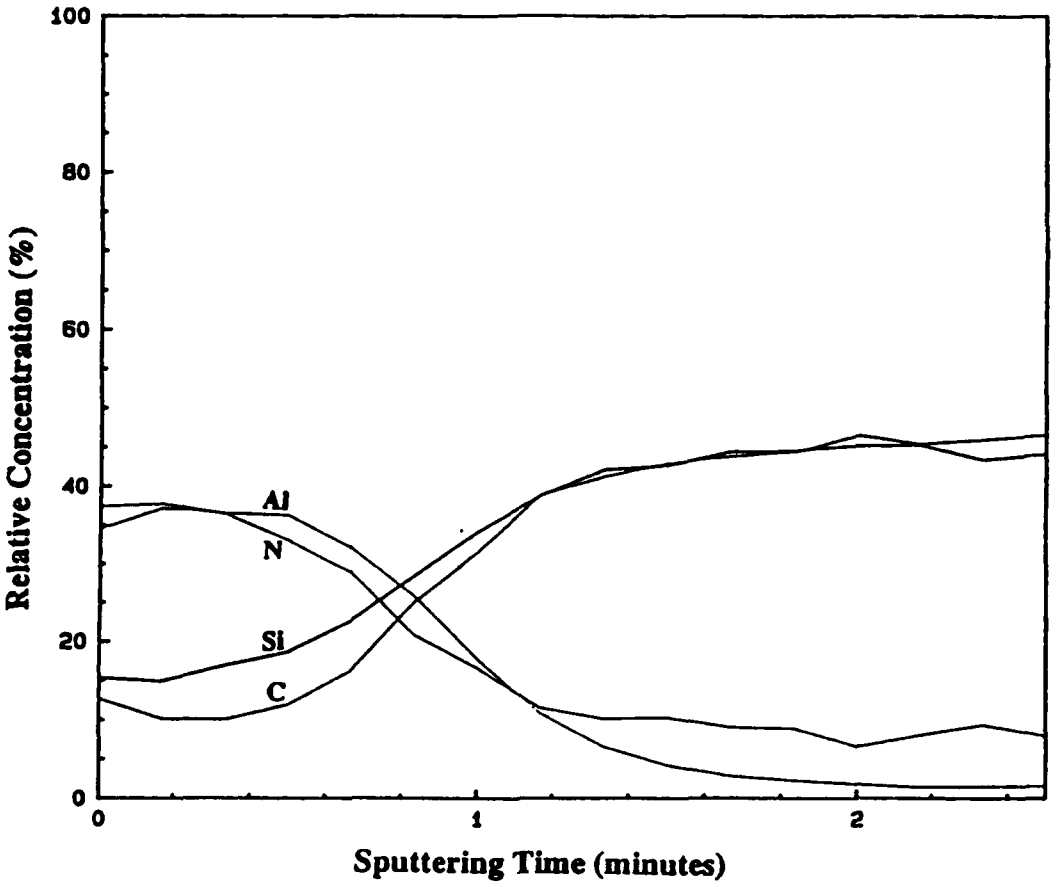

Figure 2: Auger plot of relative concentration vs. time for an AlN-SiC solid solution film.

2. Multilayers

Figure 3 shows an HRTEM image of a layer of AlN grown onto a 6H-SiC substrate. The inset of the photograph shows a diffraction pattern for the AlN region. The diffraction pattern identifies this AlN layer as being a single crystal, wurtzite (2H) structure. Note that the AlN surface appears very wavy and rough.In addition, the film-substrate interface is very disordered. Obviously, this layer would not be satisfactory for multilayer thin films.

In an attempt to improve film quality, further studies were done to find the optimum temperature for multilayer growth. This was found to be 1050°C and Figure 4 shows an Auger plot of such a multilayer. The SiC is found to be stoichiometric and about 160 Å thick. The relative concentrations of Al and N in the AlN layer correspond well to those obtained from a standard for AlN that was shown in the previous report indicating it to be stoichiometric. This layer is about 70 Å thick.

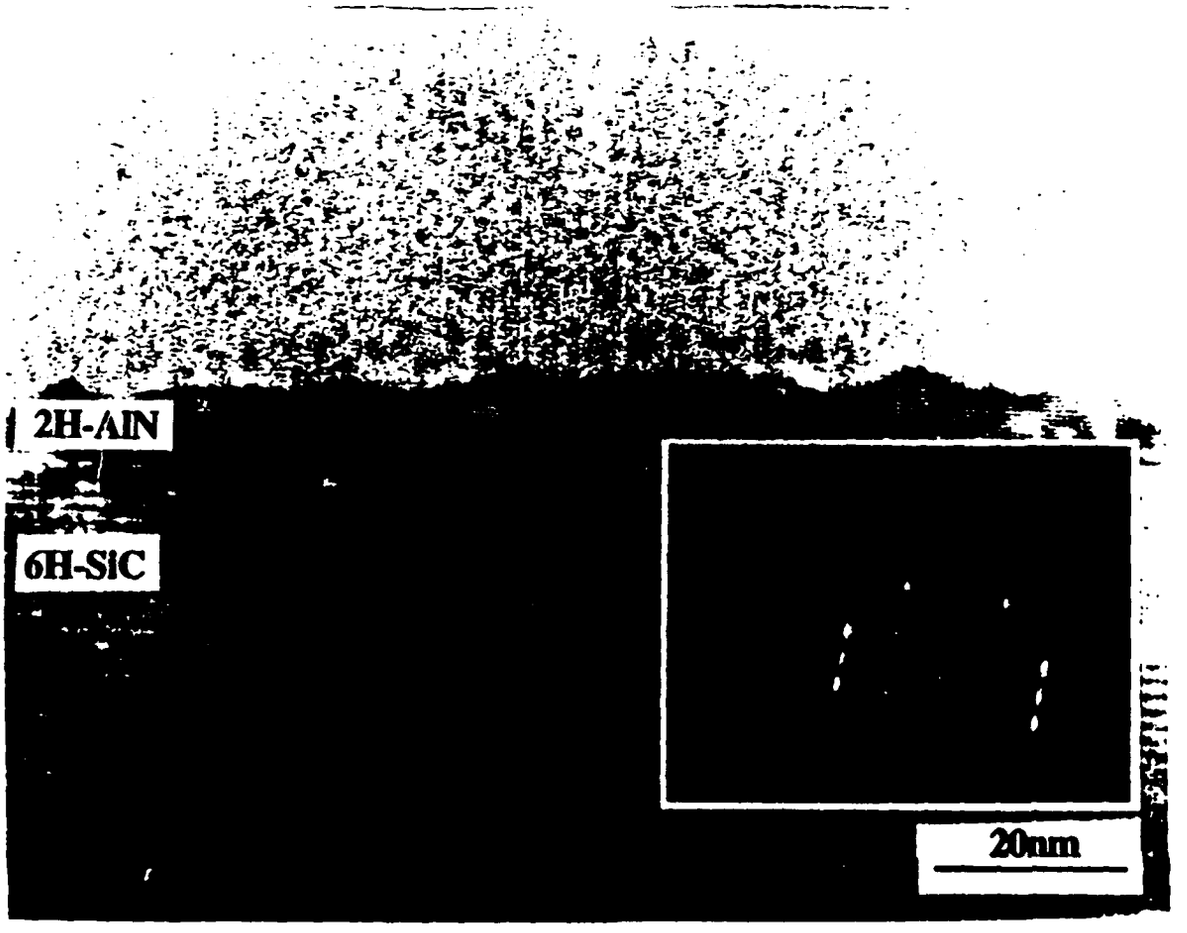

Figure 3: Cross-sectional HRTEM image of 2H-AlN film and 6H-SiC substrate Inset: Diffraction pattern for the AlN layer indicates a 2H (wurtzite) structure.

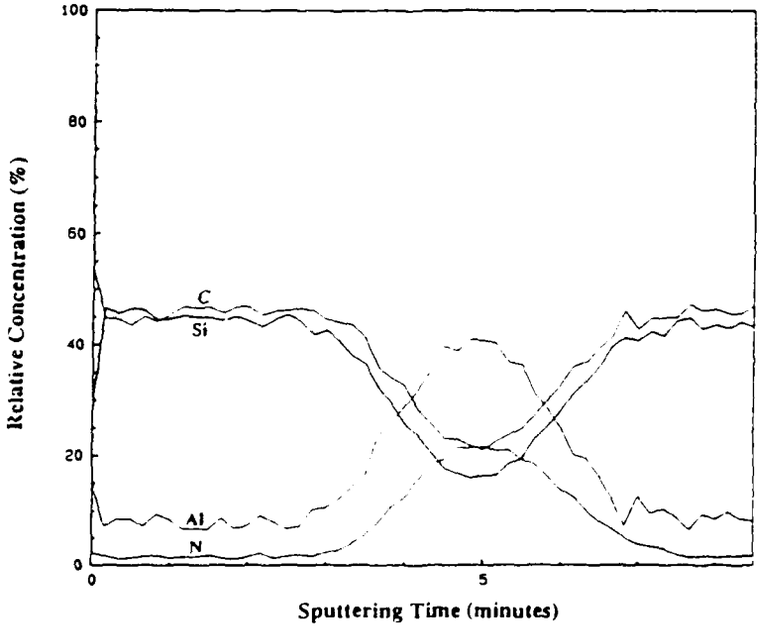

Figure 4: Auger plot of relative concentration vs. time for an AlN-SiC multilayer.

Figure 5 shows a RHEED photograph of the top (SiC) layer of this heterostructure taken after growth. The pattern is characteristic of a $[2\bar{1}\bar{1}0]$ zone axis in the cubic system.The pattern also indicates that the SiC layer is a single crystal. Refer to Figure 3 for the diffraction image of 2H-AlN.

Figure 6 shows the surface morphology of the SiC top layer. The surface appears very smooth except for widely spaced, faceted imperfections 0.5-1.0 μm across. The remaining film appears smooth at high magnification.

An HRTEM photograph of this multilayer is shown in Figure 7. There are three structures present in the layering scheme--3C- and 6H-SiC and 2H-AlN. The interface between the substrate and the AlN layer is far superior to that shown in Figure 3. This interface is good except around the surface stepson the substrate. At these steps, there is a strain field that perpetuates itself throughout the film as noted by the contrast around the steps in the photograph. The actual AlN later shows a much better thickness uniformity than the layer shown in Figure 3 grown 150°C higher. The interface between the 2H-AlN and the 3C-SiC layers is also very good. However, the SiC layer itself shows stacking faults, microtwins, and poor thickness uniformity.

Figure 5: RHEED image of an AlN-SiC multilayer on a 6H-SiC substrate taken after growth.

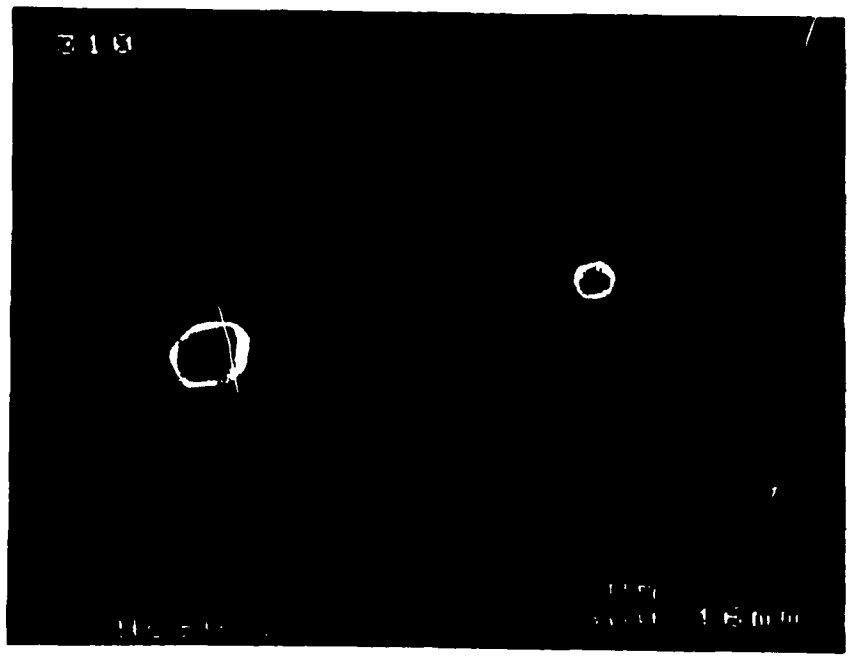

Figure 6: Surface morphology of the top layer (SiC) of a multilayer film by scanning electron microscopy

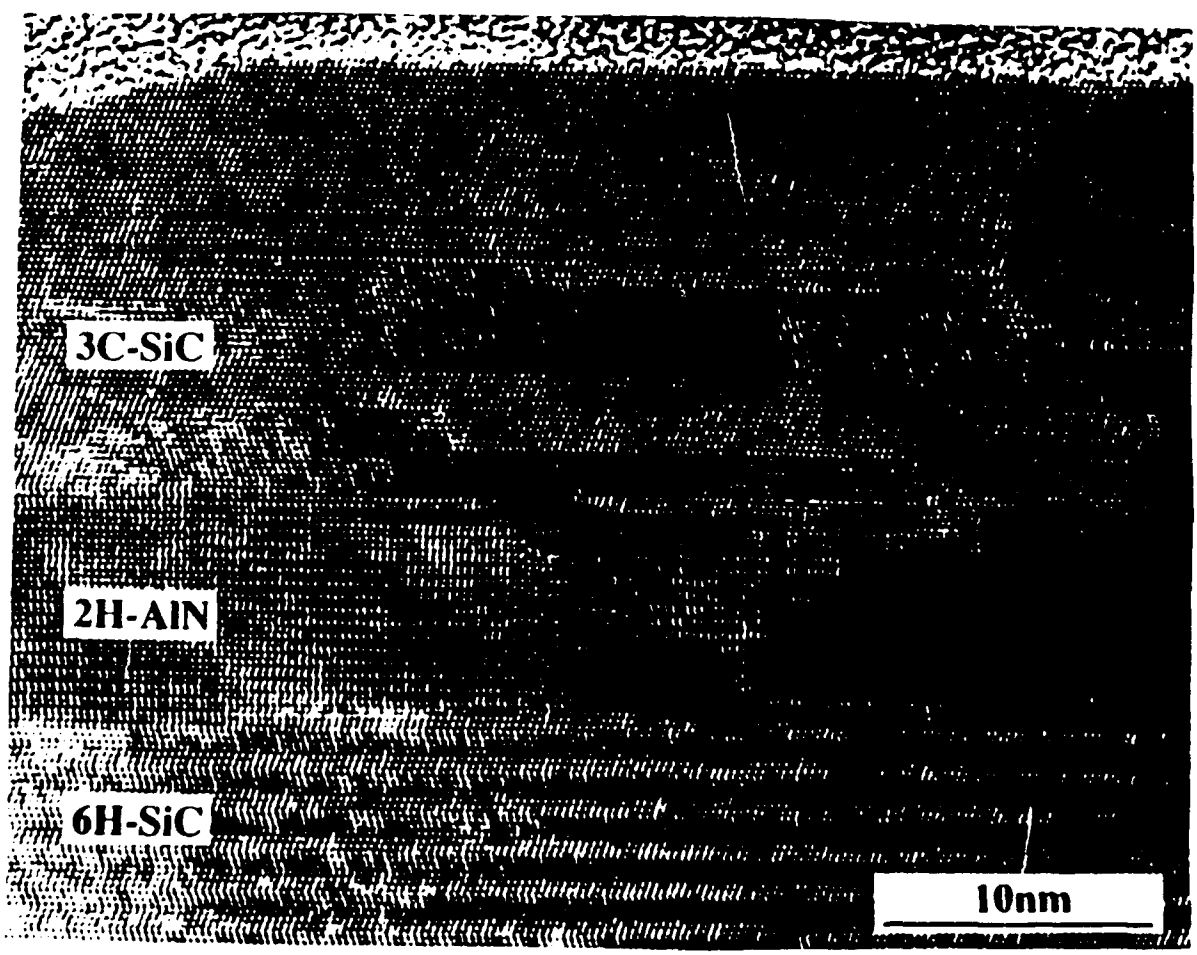

Figure 7: Cross-sectional HRTEM image of a multilayer with a 6H-SiC substrate, a 2H-AlN film, and a 3C-SiC film.

C. Discussion

1. Solid Solutions

As shown in Figures 1 and 2, the solid solutions grown are AlN-rich, have a cubic crystal structure, and are polycrystalline. To the knowledge of the authors, this is the first cubic thin film solid solution in the $(AlN)_X(SiC)_{1-X}$ system. However, the polycrystalline nature of the film and the thinness prevent further characterization and analysis. Several techniques are presently being studied to improve the crystalline character of the films as well as the growth rate. This study should address all the variables in the growth procedure. In addition, the relative difficulty of carbon incorporation in these films must also be addressed. This is also being studied.

2. Multilayers

When the initial work was done on SiC (see previous reports), the optimum growth temperature was reported to be 1200-1250°C. These conditions were then attempted for AlN growth. The results are shown in Figure 3. The films showed poor interface and surface characteristics as described previously. The disordered interface can be lessened by holding the substrate for less time at temperature, thereby lessening any Si evaporation and/or surface roughening, and eliminating pre-exposure by the N_2 plasma which may result in Si_3N_4 formation. The rough interface indicates that the growth temperature is too high.

With these concerns in mind, the heterostructure shown in Figures 4 through 7 was grown. The substrate temperature 1050°C (150°C lower), the substrate was not held at temperature for an extended period, and the substrate surface was carefully exposed to both Al and N to prevent Si_3N_4 formation at the interface. In addition, the SiC layer was grown at 1050°C.

As mentioned in the Introduction, many researchers have reported the growth of AlN on SiC substrates or SiC on AlN substrates. However, to the authors' knowledge, there has never been a report of a multilayer grown between these two materials as is presented here. In addition, there are no known reports of heterostructure growth where the first three layers (substrate included) each had a different crystal structure as presented here. This unique structure, made of direct (AlN) and indirect (SiC) wide bandgap materials, will have interesting mechanical, thermal, and electrical properties that should be studied. Also, the structure of the layers beyond those grown here will produce many interesting results. Future work is planned in these areas.

D. Conclusions

Cubic solid solutions of AlN and SiC were grown on off-axis 6H-SiC (0001) substrates by GSMBE. Although the films are polycrystalline, they represent the first thin film solid

solutions in the SiC-AlN system. With better control and precision, single crystal films of high quality should be obtained.

The first AlN-SiC multilayer reported has also been presented and described herein. The layers of AlN and SiC are both single crystal and the interfaces are of good quality. A new substrate temperature, in the range where smooth, single crystal AlN can be grown, was found to produce single crystal SiC films. This multilayer is also the first reported to include three different crystal structures in its layers. With a smoother SiC surface, this structure can easily be extended to include more layers and even begin designing devices to exploit the structure properties.

E. Future Research Plans/Goals

Additional studies are planned to study the effect of substrate temperature on both the solid solutions and the multilayers. The resulting films will be analyzed chemically, structurally, and electrically to determine properties. Devices fabricated from pure materials, doped materials, solid solutions, and multilayers will also be studied.

IV. Deposition and Characterization of Ti, Pt and Hf Rectifying Contacts on n-Type Alpha (6H)-SiC

A. Experimental Procedure

Vicinal single crystal, nitrogen-doped, n-type (10^{16} - 10^{18} cm^{-3}) substrates of 6H-SiC (0001) containing 0.5-0.8 μm thick, nitrogen-doped (10^{16} cm^{-3}) homoepitaxial films were provided by Cree Research, Inc. The Si-terminated (0001) surface, tilted 3°-4° towards [11$\bar{2}$0] was used for all depositions and analyses.

For processing Ti contacts substrates were cleaned in sequence using a 10 min. dip in an ethanol / hydrofluoric acid / deionized water (10:1:1) solution and a thermal desorption in ultra-high vacuum (UHV) (1 - 5×10^{-10} Torr). All processing steps were the same for Pt and Hf contacts, except 10% HF in deionized water was substituted for the wet chemical clean. A resistive graphite heater was used to heat the substrates at 700°C for 15 min. X-ray photoelectron spectroscopy (XPS), accessible by UHV transfer from the heating station and deposition chamber, was used to monitor surface chemistry and structure, respectively. The XPS system consisted of a Riber Mac2 semi-dispersive electron energy analyzer and a Riber pulse counter. A Mg anode was used at 1.2 eV resolution for obtaining valence structure and 0.8 eV resolution for core level data. The metals were deposited onto unheated substrates by electron beam evaporation (base pressure < 2×10^{-10} Torr). The first 10 nm was deposited at a rate of 1 nm/min. The deposition rate was then increased to 2 - 3 nm/min. to give a total thickness of 100 nm. For electrical characterization vertical contact structures consisting of 500 μm and 750 μm diameter circular contacts were created by depositing the metal through a Mo mask in contact with the (0001) SiC epitaxial layer, leaving a patterned metal film. Conductive liquid Ag served as the large area back contact. All subsequent annealing was done in UHV. Current-voltage (I-V) measurements were taken with a Rucker & Kolls Model 260 probe station in conjunction with an HP 4145A Semiconductor Parameter Analyzer.

Capacitance-voltage (C-V) measurements were taken with a Keithley Model 5956 Package 82 Simultaneous CV System in conjunction with an HP vector PC-308. The contact structures were the same as above. Measurements were taken at a frequency of 1 MHz.

Ti/SiC samples were prepared in cross-section for TEM analysis. High resolution images and selected area diffraction patterns were obtained with an ISI EM 002B operating at 200 kV.

B. Results

1. Ti Contacts

In our December, 1991 Annual Letter Report we reported epitaxial growth of Ti contacts, which were found to be rectifying with typical leakage currents at -10 V of 6 nA (1×10^{-7} A/cm^2). Barrier height values of 0.88 eV for as-deposited and 1.04 eV for annealed Ti/SiC were calculated from differential capacitance measurements as a function of reverse voltage.

Notably low ideality factors in the range 1.01 - 1.09 were calculated from plots of log I vs. V. In addition, these contacts were found to remain stable after annealing at 700°C for 1 hour.

As a comparison to the barrier height calculated by capacitance-voltage measurements, an alternative method using x-ray photoelectron spectroscopy (XPS) was employed. The low binding energy region of the spectrum (0 - 30 eV) gives the valence structure from which a valence band maximum may be determined.

The valence structure of the 'clean' SiC surface is shown in the lower part of Figure 1. The valence band edge is marked E_V in the diagram and was located by extrapolating the prominant leading edge of the valence spectrum. As can be seen, there is some uncertainty in locating the highest filled electron level. The tailing of the electron distribution may due to the finite width in the system resolution and/or surface contamination, i.e. oxygen adsorption. The estimated 5.5 eV value of the valence band edge must be compared to the Fermi level at 3.9 eV (This is the workfunction of the spectrometer.) to have any relative meaning. In other words, the Fermi level at the surface is located 1.6 eV above the valence band. For a bandgap of 2.86 eV, this corresponds to a 1.3 eV difference between the conduction band and the Fermi level (see Fig. 2). However, because the semiconductor has a carrier concentration of 1×10^{16} cm^{-3}, the difference between the conduction band and Fermi level in the bulk of the semiconductor must be 0.18 eV. This difference between the relative energy bands in the bulk material and at the surface implies that the Fermi level is pinned at the surface near midgap.

The other spectra in Figure 1 were taken after successive depositions of 2 Å of Ti onto the SiC surface. With a thin metal overlayer there should be electron occupancy up to the Fermi level with a corresponding energy shift in the valence band of the semiconductor. However, there appears to be no shifting in the valence structure of the SiC. Therefore, the barrier height at the Ti/SiC interface is deduced to be equal to 1.3 eV, which was the difference between the conduction band and Fermi level before Ti deposition.

2. Pt Contacts

Platinum contacts as-depostied at room temperature made Schottky contacts to SiC with very low leakage currents and low ideality factors (Fig. 3). The leakage at -10 V was typically 0.10 nA (5×10^{-8} cm^2), and the ideality factors calculated from log I vs. V (Fig. 4) were between n = 1.04 - 1.06.

After obtaining measurements of as-deposited Pt contacts, the contacts were annealed in ultra-high vacuum. Successive 20 minute anneals at 450°C and 550°C yielded no detectable differences in the leakage in the current-voltage characteristics. However, an additional 20 minute anneal at 650°C resulted in degradation of the characteristics (Figs. 3 and 5).

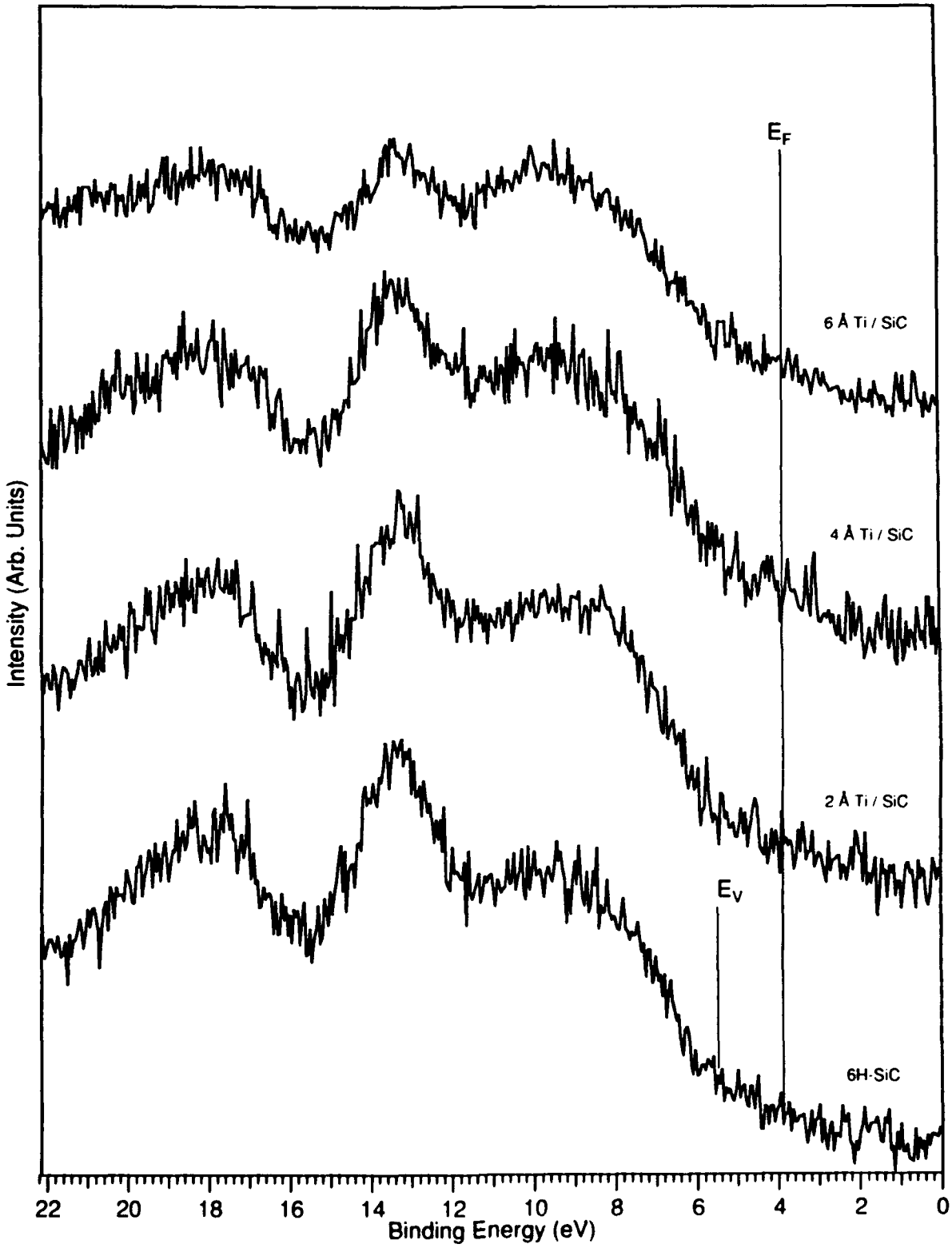

Figure 1. XPS valence structure of (0001) 6H-SiC both before and after 2 Å layer deposition series of Ti.

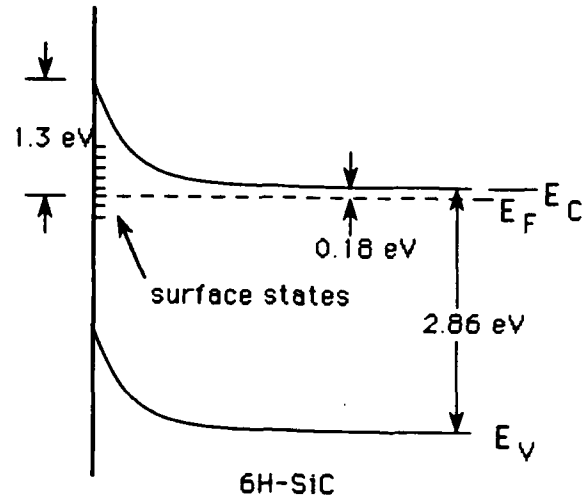

Figure 2. Schematic band diagram of (0001) 6H-SiC.

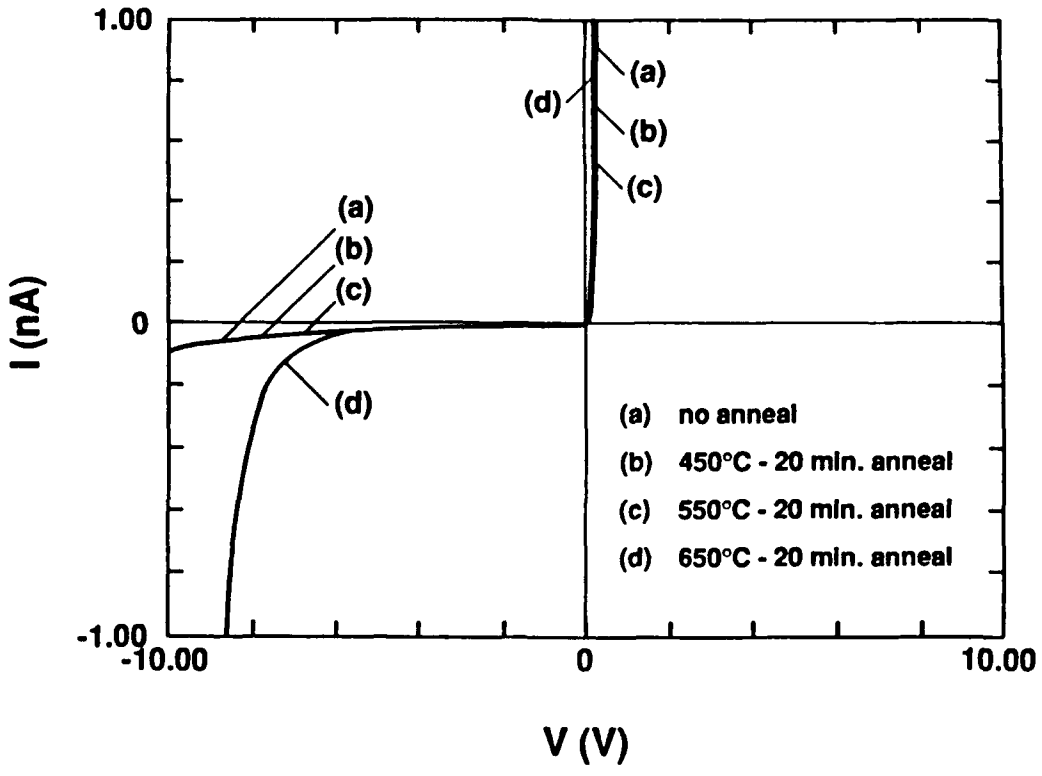

Figure 3. Current-voltage characteristics of Pt deposited on (0001) 6H-SiC epitaxial layer. (2.0×10^{-3} cm^2 contact area).

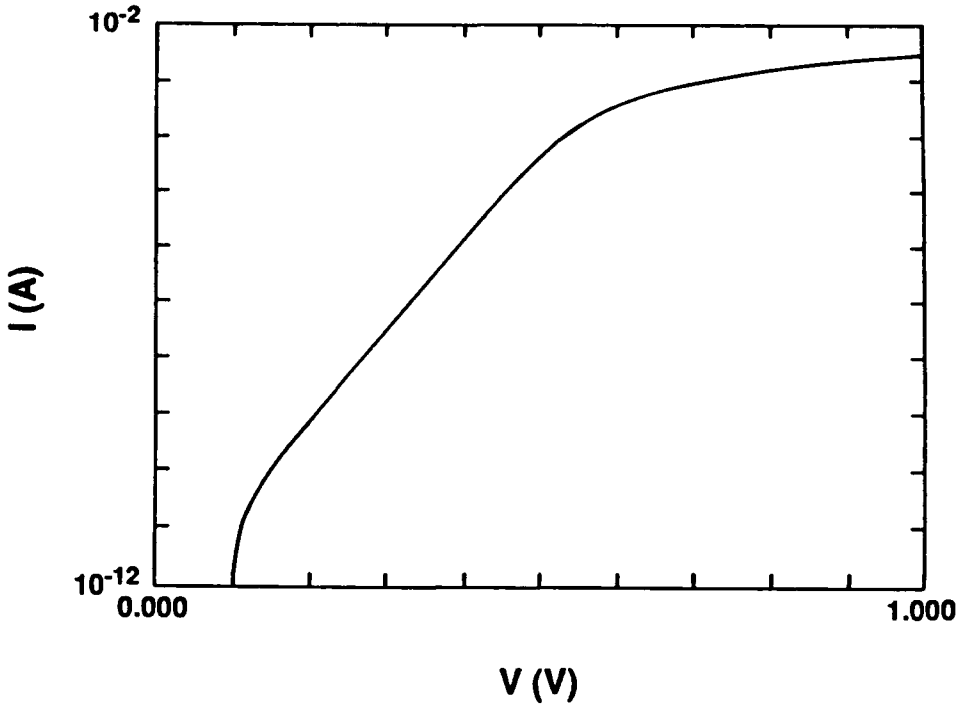

Figure 4. Log I vs. V of Pt deposited on (0001) 6H-SiC. n = 1.06 +/- .02.

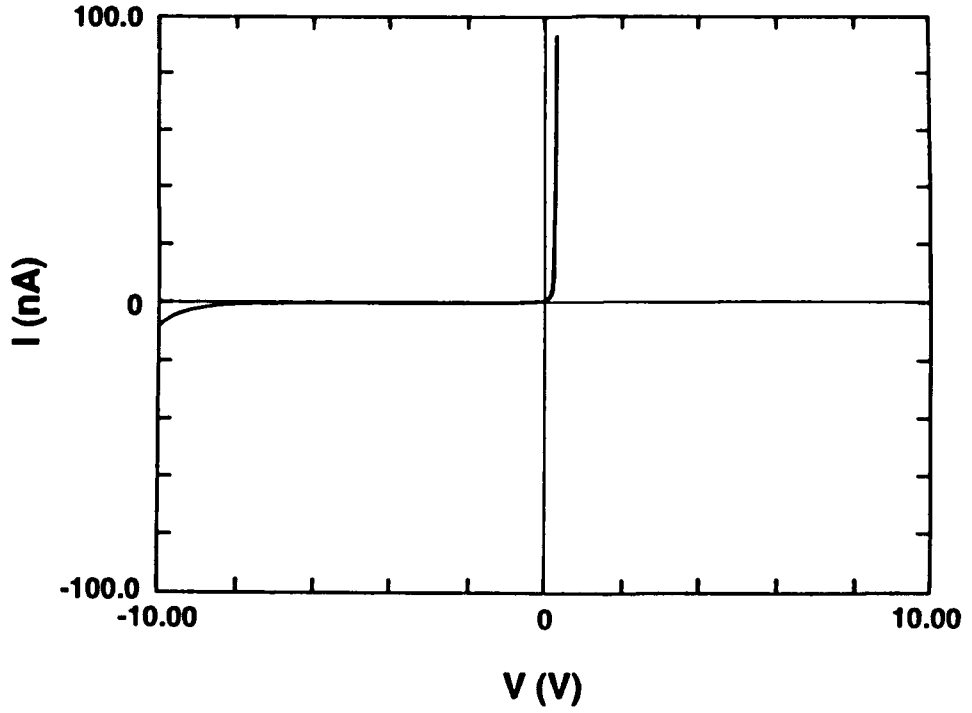

Figure 5. Current-voltage characteristics of Pt/6H-SiC after annealing at 650°C for 20 min. (2.0×10^{-3} cm^2 contact area).

With low ideality factors and high slopes in log I vs. log V plots (Fig.6), a necessary condition for current transport by thermionic emission [1], the barrier height may be calculated [2]:

$$\Phi_B \equiv \ln \frac{A^{**}T^2}{J_S},$$

where A** is Richardson's constant and J_S is the extrapolated value of current density at zero voltage. The extrapolated value was taken from the linear region of the log I vs. V plot shown in Figure 4. For 6H-SiC a calculated value for Richardson's constant is A** = 194.4 A/cm^2K^2 (private communication with John Palmour, Cree Research, Inc.). Following through with this calculation gives Φ_B = 1.01 V for as-deposited Pt contacts. This value is in excellent agreement with the 1.02 V value calculated from capacitance-voltage measurements and reported in the Dec., 1991 Annual Letter Report. Similar calculations were carried out for the annealed contacts. A slight increase in the barrier height to 1.05 V occurred after the 550°C anneal; however, a barrier height could not be calculated for the 650°C annealed contacts.

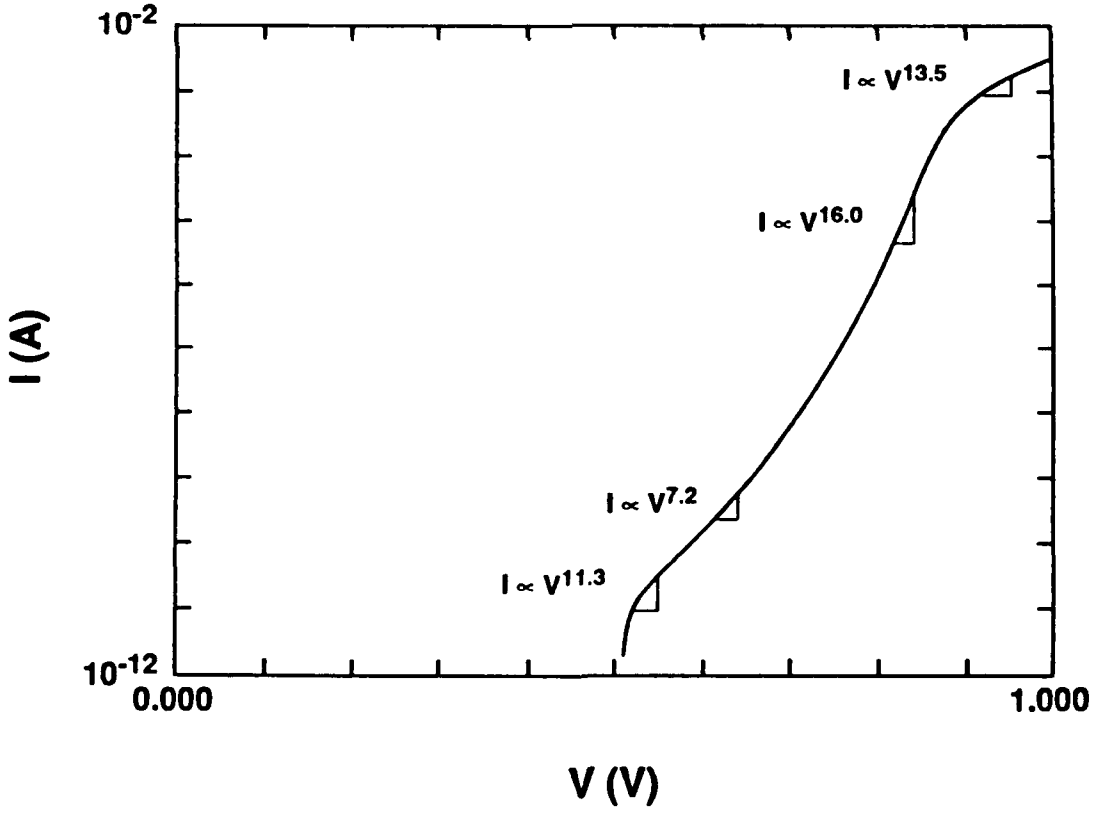

Figure 6. Log I vs. Log V of as-deposited Pt/SiC.

3. Hf Contacts

Current-voltage measurements of as-deposited and annealed hafnium contacts also displayed rectifying characteristics. The as-deposited contacts produced typical leakage currents of 2.5×10^{-7} A/cm^2 at -10 V, while annealing at 700°C for 20 minutes resulted in a reduction of the leakage to 4.0×10^{-8} A/cm^2 (Figs. 7 and 8). Figure 7 shows that the characteristics improved for the first 20 minute anneal, but then degraded again with subsequent 20 min. anneals up to a total anneal time of 60 minutes.

The log I vs. V plots in the forward region show consistent values of ideality factors between 1.04 - 1.06. As for the Pt contacts, the linear regime extended over four decades of current, and high slopes resulted from plotting log I vs. log V.

In correlation with the observable variation in the reverse characteristics with annealing time, examination of the log I vs. V plots shows a change in the barrier height as the interfacial reaction proceeds. A J_S value of 1.0×10^{-9} A/cm^2 was determined which results in a calculated barrier height of 0.97 V for the unannealed contact. By similar calculations, the barrier increased to 1.01 V after the 20 min. anneal and then successively decreased to 0.93 V and 0.86 V for the 40 min. and 60 min. anneals, respectively. Qualitatively, the leakage current appears to vary inversely with the height of the barrier, as would be expected.

C. Discussion

Titanium, platinum, and hafnium deposited onto unheated, n-type 6H-SiC substrates have each formed Schottky contacts but have differences in their respective barrier heights, in the details of the current-voltage characteristics, and in the effects of annealing. A compilation of barrier heights, both measured and theoretical, is displayed in Table I.

The theoretical barrier heights for the pure, as-deposited contacts are based on the Schottky-Mott limit for ideal behavior. In this limit barrier height equals the difference between the workfunction of the metal and the electron affinity (measured from the conduction band edge to vacuum) of the semiconductor. The electron affinity was calculated to be 3.37 eV by taking the intrinsic workfunction to be 4.80 eV [3] and assuming that the bands remain flat at the surface. However, this situation exists only if the Fermi level is not pinned at the surface by surface states or other effects. L.J. Brillson [4] explains that interface dipoles which can pin the Fermi level can also accomodate charge on forming the metal-semiconductor contact. This results in a barrier height which is independent of the metal contact. For device applications this result is undesirable, because one wants to have flexibility in controlling the contact characteristics, specifically when trying to form ohmic and Schottky contacts.

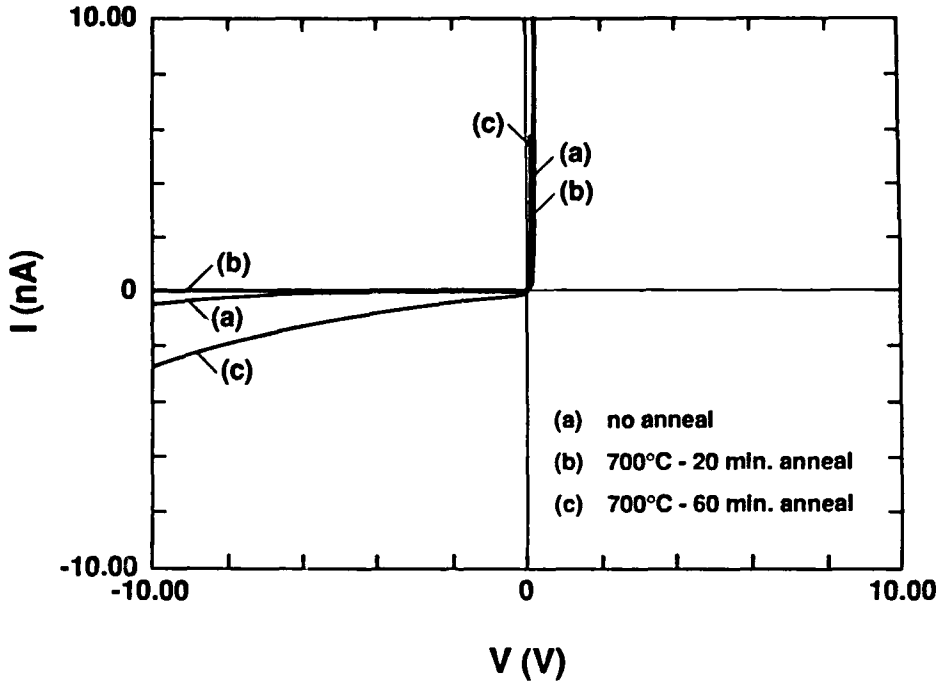

Figure 7. Current-voltage characteristics of Hf deposited on (0001) 6H-SiC. (2.0×10^{-3} cm^2 contact area).

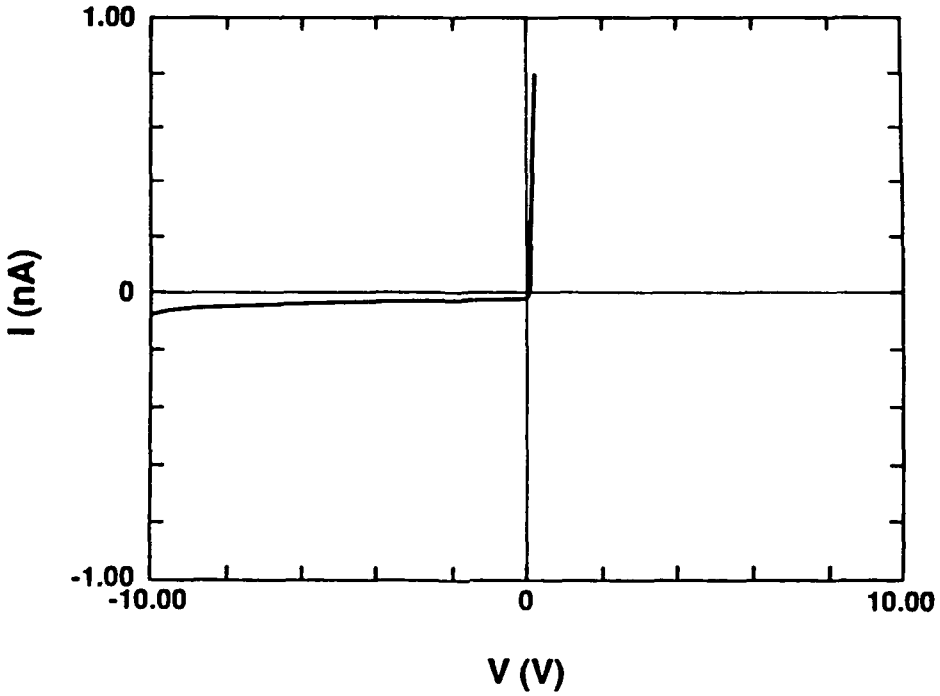

Figure 8. Current-voltage characteristics of Hf/SiC after annealing at 700°C for 20 min. (2.0×10^{-3} cm^2 contact area).

Table I. Measured and theoretical barrier heights for selected metal contacts to n-type 6H-SiC.

Metal	Φ_B^{I-V} (eV)	Φ_B^{C-V} (eV)	Φ_B^{XPS} (eV)	Φ_B^{th} (eV)
Ti (no anneal)	——	0.88	1.4	0.95
Ti (700°C, 60 min.)	——	1.04	——	——
Pt (no anneal)	1.01	1.02	——	2.27
Pt (450°C, 20 min.)	"	——	——	——
Pt (550°C, 20 min.)	1.05	——	——	——
Hf (no anneal)	0.97	0.89	——	0.52
Hf (700°C, 20 min.)	1.01	——	——	——
Hf (700°C, 40 min.)	0.93	——	——	——
Hf (700°C, 60 min.)	0.86	——	——	——

Without Fermi level pinning the barrier height for Ti contacts to n-type 6H-SiC is predicted to be 0.95 V. Table I shows that there is significant variation between the predicted barrier and the barrier measured by C-V and XPS techniques. At this point a thorough error analysis has not been performed. However, the interpretation of the XPS data appears to be susceptible to more error. First of all, the tailing of the valence spectrum (Fig. 1) causes a few tenths of an electron-volt uncertainty in locating the valence band maximum. Secondly, it is possible that slight shifting in the valence spectrum would be discerned if another Ti layer a few angstroms thick had been deposited. A large part of this research effort will be devoted to comparing several measurement techniques and to reducing the amount of error introduced in the interpretation.

After annealing the Ti contacts for 60 min. at 700°C, capacitance-voltage measurements indicate that the barrier has increased. From TEM analysis we reported the formation of TiC particles in a matrix of Ti_5Si_3 (Dec. 1991 Annual Letter Report). The properties of the annealed interface should then be determined by the Ti_5Si_3/SiC contact.

Similar TEM analysis will be performed on Pt/SiC contacts and correlated with electrical measurements which have been taken. As described in detail above, as-deposited Pt contacts showed excellent rectification behavior (Fig. 3). In addition, the barrier heights calculated from current-voltage and capacitance-voltage measurements are in excellent agreement with eachother. However, theory predicts a much higher barrier than what is measured. This descrepancy gives further evidence that the Fermi level is pinned at the SiC surface.

Not only does there appear to be a smaller measured barrier, at the 1.0 eVrange, than the predicted barrier (as for Pt contacts), but there is also an increase in the measured barrier over the predicted barrier to approx. 1.0 eV for Hf contacts (Table I). If indeed the Fermi level is pinned for the as-deposited contacts, chemical reaction upon annealing in effect unpins it. In fact an interesting trend falls out of the analysis of the Hf/SiC annealing series. After an initial anneal at 700°C for 20 min., the barrier height increases slightly (Table I). However, additional annealing results in decreasing the barrier. A high barrier should result in a better Schottky contact, wheras a lower barrier should result in degradation of the current-voltage characteristics; this trend is exactly what is shown in the curent-voltage characteristics of Figure 7.

D. Conclusions

Titanium, platinum, and hafnium deposited on (0001) 6H-SiC at room temperature were all rectifying with calculated ideality factors less than 1.1. Of the unannealed contacts, Pt has formed in terms of leakage current, which was 5×10^{-8} A/cm^2 at -10 V. However, after annealing Hf contacts at 700°C for 20 minutes, the leakage decreased to 4×10^{-8} A/cm^2.

The XPS valence structure of the 'clean' SiC substrate indicates that the Fermi level is pinned near midgap. Although the predicted barriers range from 0.52 eV for Hf to 2.27 eV for Pt, the measured barrier heights remained very close to 1.0 eV. This independence of the barrier height on the metal gives further evidence that the Fermi level is pinned at the SiC surface.

Changes in both the barrier height and the electrical characteristics were seen however after annealing. These changes indicate that chemical reaction overcomes the effects of Fermi level pinning and becomes the controlling factor. For example, in Ti contacts annealed at 700°C, the interface was found by TEM analysis to consist of TiC particles in a matrix of Ti_5Si_3. The electrical characteristics then become dependent on the Ti_5Si_3/SiC interface instead of the Ti/SiC interface. Similar TEM analyses will be performed on Pt/SiC and Hf/SiC interfaces.

E. Future Research Plans/Goals

An experimental setup for internal photoemission, an optical technique for measuring barrier height, has been arranged. In internal photoemission electrical contact is established to the frontside and backside contacts, and the wavelength of a monochromated light source is varied. A photocurrent is created when the energy of the light is equal to or greater than the barrier height. A xenon lamp is being used for the monochromated light source. At this time some problems (making contact to the diode, etc.) need to be worked out in order to get measurements on SiC samples.

The investigations of Pt and Hf contacts to n-type SiC will be continued. Annealing of the contacts caused changes in the electrical characteristics, which indicates that chemical reaction has occurred. Phases fromed during the annealing series will be identified and correlated with the electrical properties, both macroscopic and microscopic. In fact, if the chemical and electrical data for Hf suggest the potential for ohmicity with continued reaction, the annealing series will be extended.

An electrical, chemical, and structural study will also be initiated on Co/SiC and Sr/SiC systems. For an ideal contact, theory predicts that Sr forms an ohmic contact with SiC. On the other hand, Co should form a Schottky contact as-deposited, but may become ohmic on annealing at high temperature as occurs in Ni contacts.

F. References

1. M. A. Lampert and P. Mark, *Current Injection in Solids*, (Academic Press, New York, 1970).
2. S. M. Sze, *Physics of Semiconductor Devices*, (John Wiley & Sons, New York, 1981).
3. J. Pelletier, D. Gervais, and C. Pomot, J. Appl. **55**, 994 (1984).
4. L. J. Brillson, Surf. Sci. Rep., **2**, 123 (1982).

V. Determination of the Diffusivity of the Al, Si, N and C at the Interface of the SiC-AlN Diffusion Couple

Abstract

The chemical interdiffusion of SiC and AlN is being investigated. For the initial run, a SiC-AlN diffusion couple was heated at 1500° C for 100 hours in a N_2 environment. Scanning Auger spectroscopy was employed for the measurements of the diffusion lengths of the four elements. The diffusivity of the four elements was calculated to be $\approx 10^{-14}$ cm^2/hr, which is about four orders of magnitude lower than the previously reported results.

A. Introduction

Several attempts have been made to alloy SiC with other compounds to control the mechanical and physical properties. Single crystal growth of SiC-AlN mixtures by epitaxial techniques on the SiC platelets is one example [1]. There exists a difference in opinion among investigators about the possibility of forming solid solutions or new phases in the SiC-AlN system at high temperatures [2]. The difficulties encountered in the attempts to obtain homogeneous SiC-AlN solid solutions are known to be related to the low diffusion coefficients.

The diffusion coefficients of N in SiC have been determined to be $\approx 10^{-12}$ cm^2/s at 2550° C [3]. In hot-pressed SiC-AlN samples and in SiC-AlN diffusion couples, approximate diffusion coefficients of SiC and AlN were calculated to be 1×10^{-12} cm^2/s [4]. The corresponding activation energy was roughly estimated to be as high as 900 kJ mol, and the pre-exponential term was $\approx 10^{-8}$ cm^2/s which is an unusually high value. Thus, it was suggested that lattice diffusion of coupled SiC and AlN pairs was responsible for these high values.

Phase transformations in the SiC-AlN system have also been studied. The 3C→2H transformation was observed to proceed through a heavily faulted cubic structure which contained up to 4 % AlN [4].

In this investigation, the diffusion coefficient and the corresponding activation energy for the diffusion of the four elements Si, C, Al, and N in the interface layer between the single crystal SiC and sintered AlN materials will be determined. Although the diffusion coefficients for N in SiC at high temperature have been determined previously, the atomic behavior and phase formation at relatively low temperature for thin film deposition have not been yet clarified For this experiment, Auger spectroscopy and TEM will be employed to determine the nature and extent of the diffusion profiles and the existence (or lack of it) of additional phases in the solid solution region and at the interfaces between the solution and the end-member phases.

B. Experimental Procedures

A SiC sample was prepared from a single crystal wafer manufactured by Cree Research, Inc. The AlN sample was prepared from sintered bulk material. The SiC wafer was used in the as-received condition, since the surface was already polished. The preparation of the AlN specimen was performed using a lapping machine in which the sample is rotated on the glass plate. For the lapping of the sample, 30 micron, 6 micron 1 micron and 0.1 micron diamond slurries were used. The polished surface of the SiC and AlN was joined just before setting into the furnace for the diffusion. The sample is heated initially to 1150°C and held there for 30 minutes under a pressure of 20 psi. After releasing the load, the temperature of the furnace is raised to 1500°C. After the diffusion anneal, the sample was lapped at an angle of 34° to determine the scanning concentration profile by Auger spectroscopy. This produced a magnification of the interface between the two materials of ≈100 times. Depth concentration profiles were taken on an island of the SiC remaining on the AlN layer. The difference in the reflectivity of the two materials makes it easier to determine the interface area in the Auger equipment.

C. Results

The depth profiles of the concentration of the four elements for this initial sample are shown in Figure 1. The data in Figure 1 are too inaccurate to calculate the diffusivity of the four elements. This is due to the rough interfaces and surface of the sputtered area. All the profiles in the Figure 1 are as expected except the oxygen profile. Oxygen is not expected to be present in the SiC or AlN materials. However, the concentration of the oxygen increases toward the AlN side. The oxide film is formed on the angle lapped surface of SiC. With ion sputtering of the surface, the oxide layer is easily eliminated, as can be seen in the Figure 1. In order to confirm this concentration depth profile, line scanning across the diffused region was conducted as the results can be seen in Figures 2–5. Using these data from the depth profiles, the diffusivity of the four elements near the interface of the SiC and AlN can be roughly estimated using the equation:

$$c(x,t) = (c/2)\,[\,1 - \mathrm{erf}\,\{x / 2\,(Dt)^{1/2}\}\,] \quad (1)$$

The results of this calculation are shown in the Table I. In this calculation, the diffusivity is assumed to be constant. However, as can be seen in the Table I, the diffusivity seems to be varied depending on the position. The diffusivities calculated in this preliminary experiment are about four orders of magnitude lower than the results of Zangvil or Vodakov.

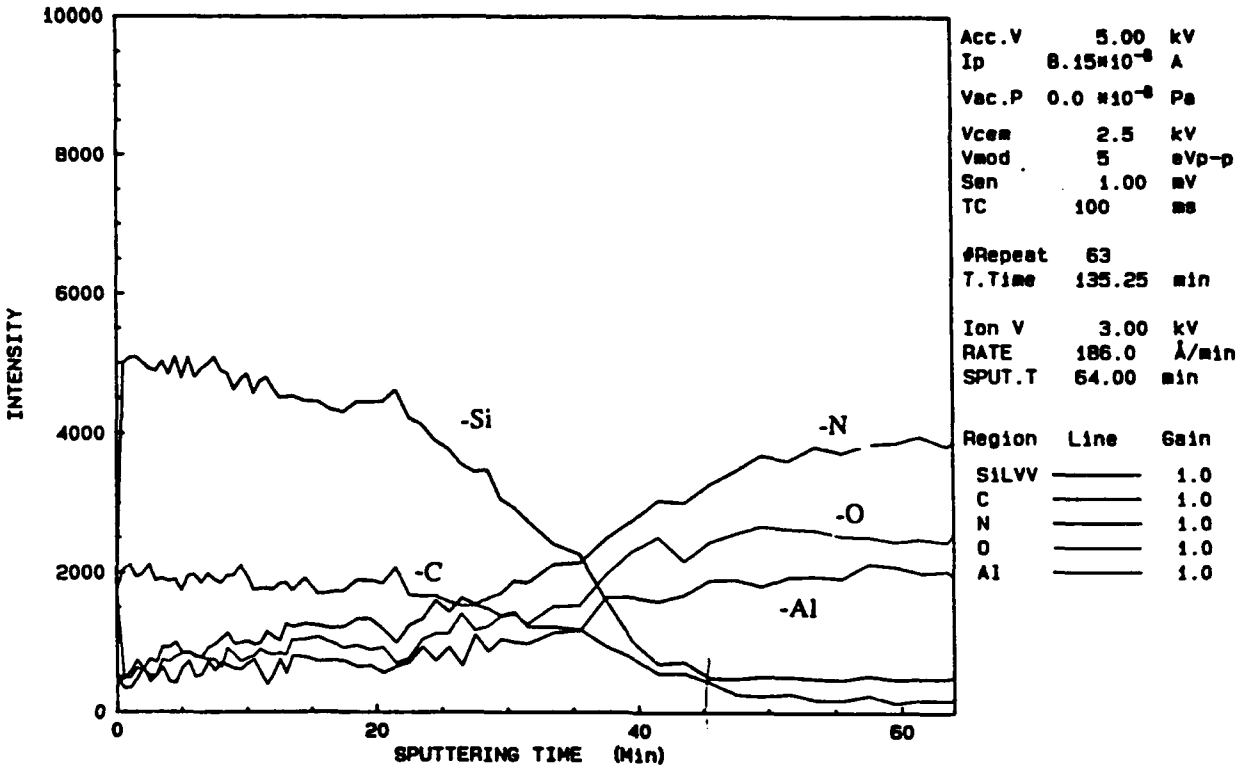

Figure 1. Depth concentration profile at the interface of SiC and AlN.

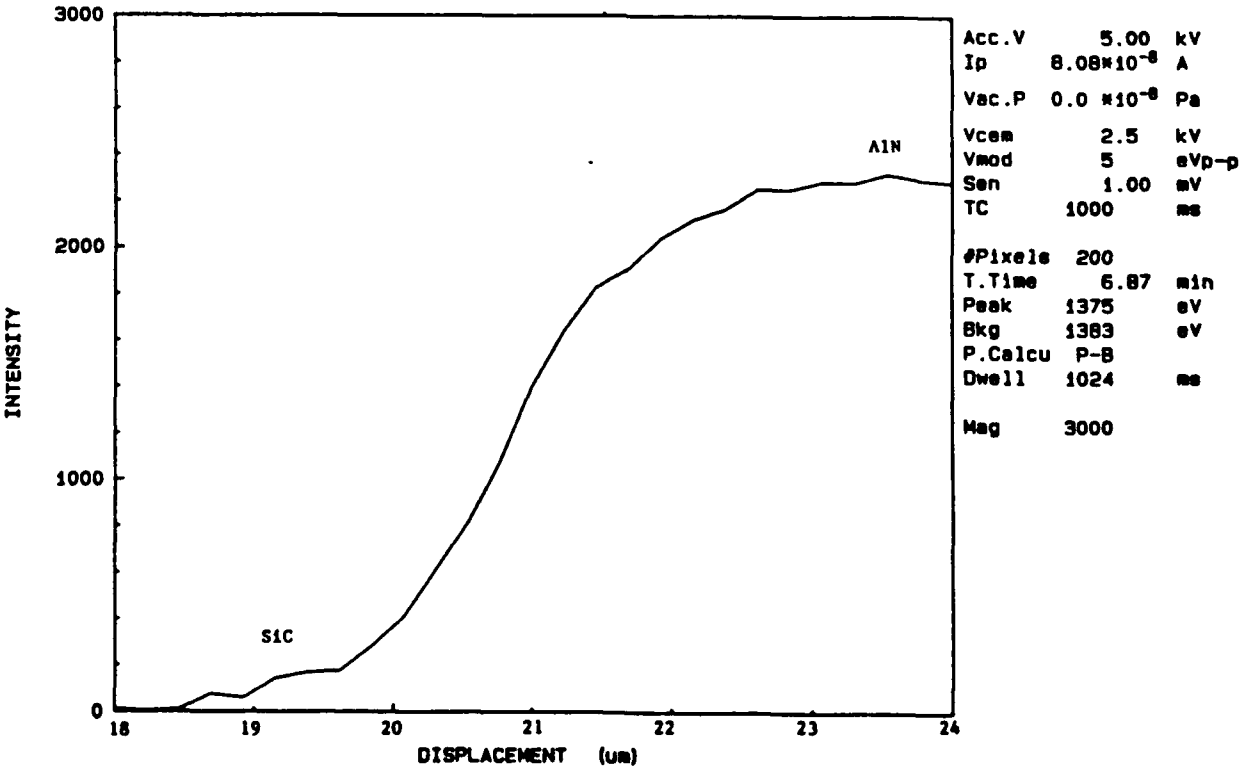

Figure 2. Line scanning of the Al concentration at the interface of SiC and AlN.

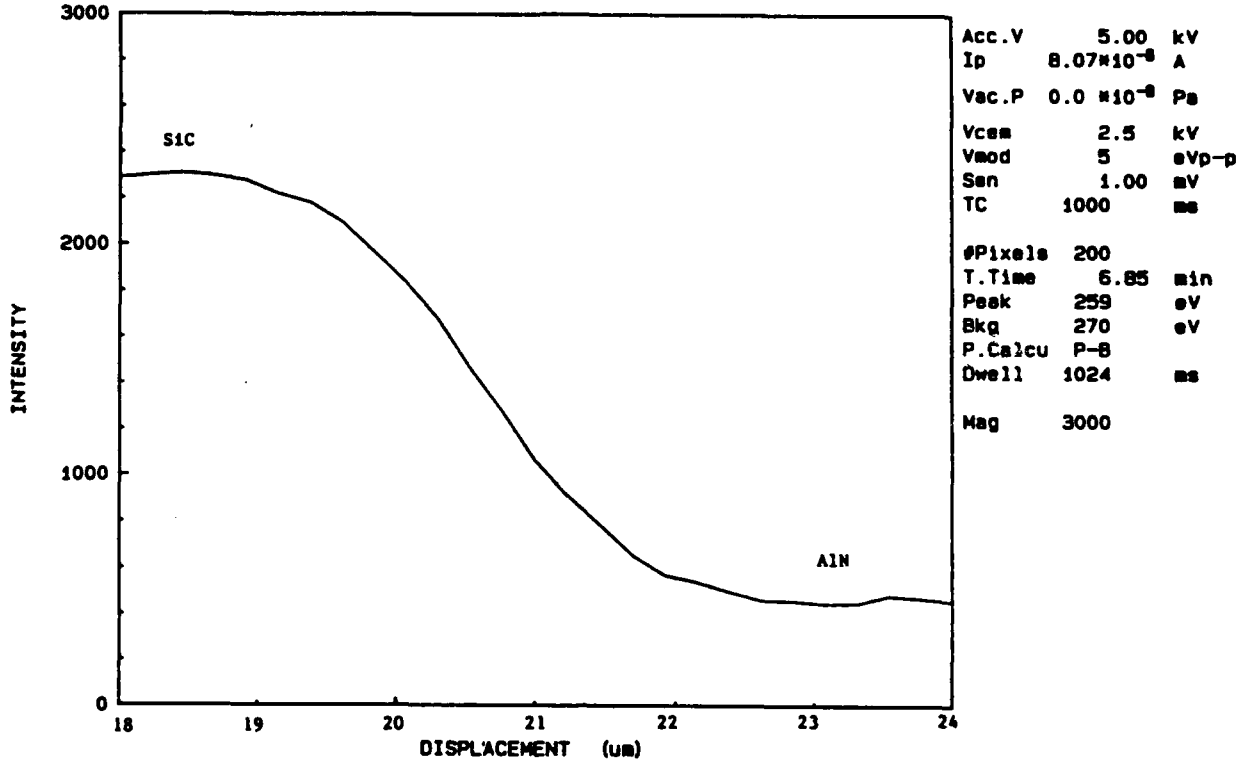

Figure 3. Line scanning of the C concentration at the interface of SiC and AlN.

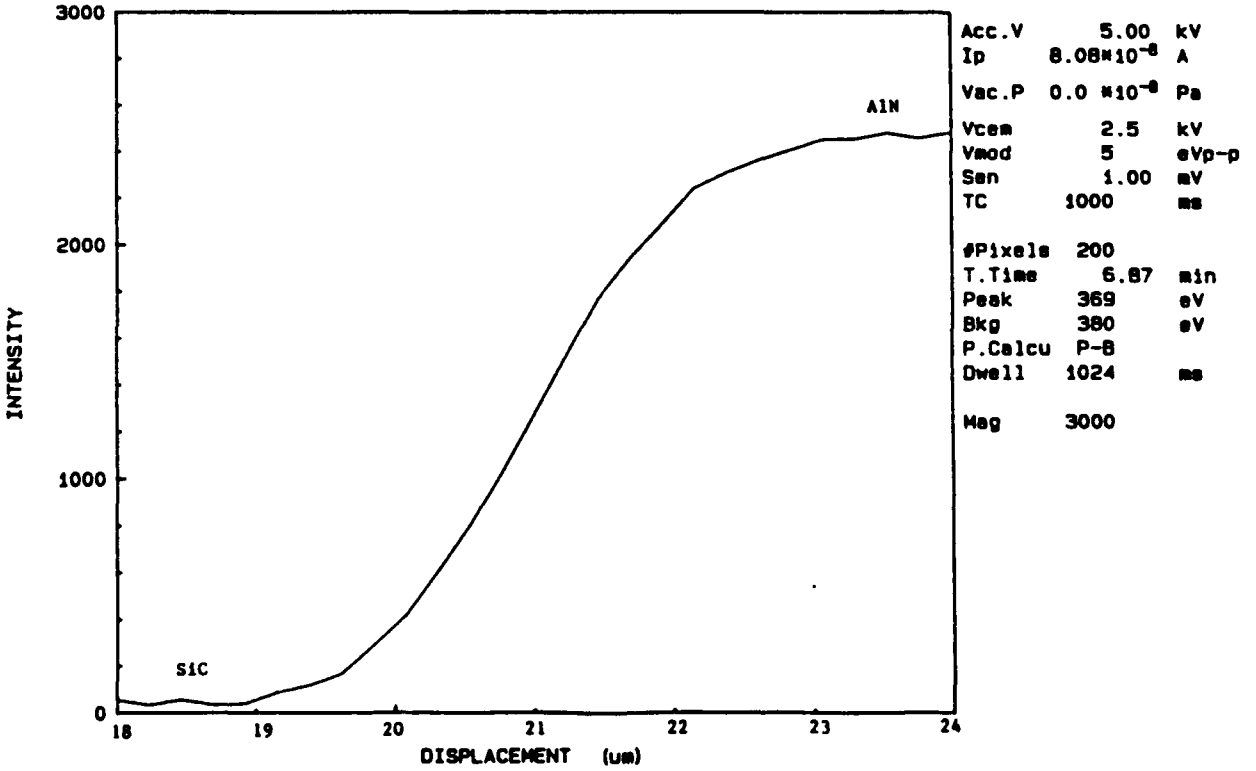

Figure 4. Line scanning of the N concentration at the interface of SiC and AlN.

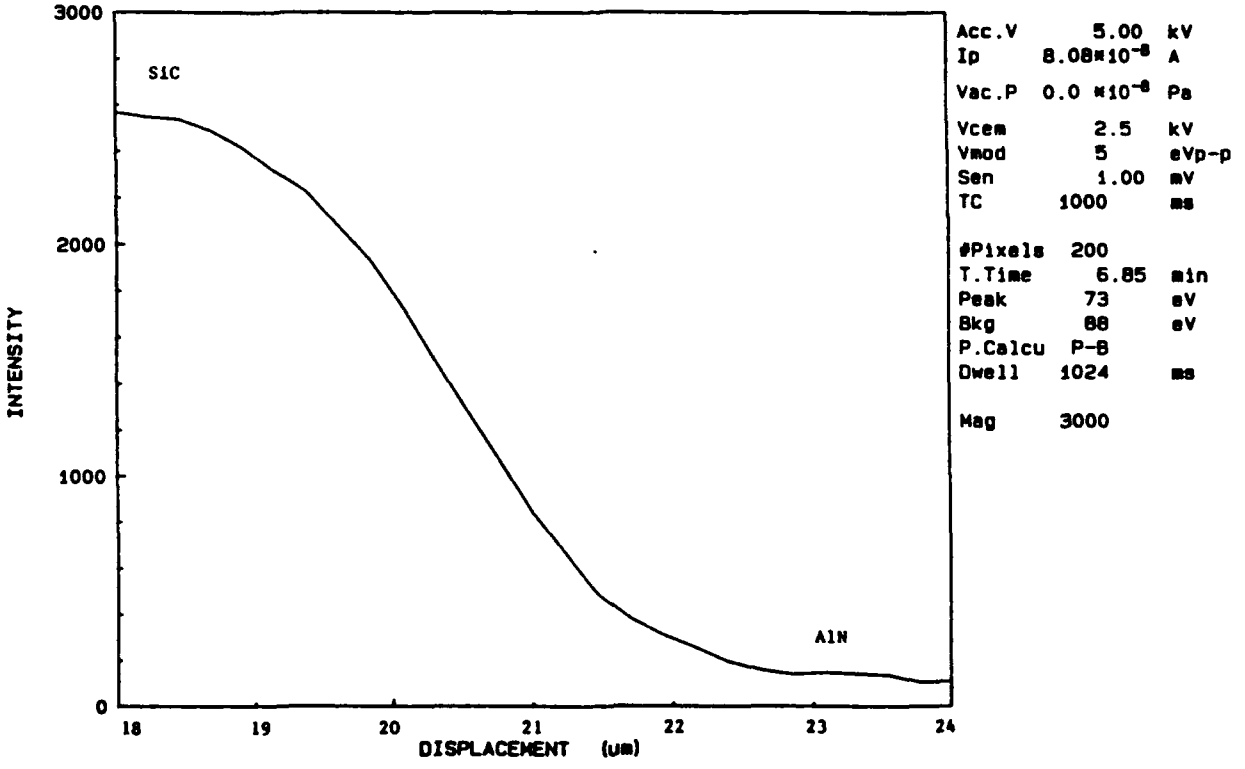

Figure 5. Line scanning of the Si concentration at the interface of SiC and AlN.

Table I.

Diffusivity (10^{-14} cm ^{2} / hr)	in AlN	in SiC
Silicon	7.96	8.4 -8.6
Carbon	6.7 - 7.3	.4-4.7
Aluminum	11	5.29
Nitrogen	6.8	5.76-6.76

D. Discussion

As can be seen in Figure 1, the depth concentration profile is too rough for the determination of the diffusivity. This may be due to the poor preparation of the raster by the ion gun. It indicates that the sputtered area should be larger and sufficiently flat for more accurate measurement of the depth profile of the concentration. The actual sputtering rate in SiC and AlN should be measured at the same time. Once an accurate depth profile is obtained, it seems to be very useful to estimate the diffusion depth. As can be seen in Figure 6, the angle-lapped interface of the AlN and SiC is not so sufficiently smooth to obtain concentration profiles by

scanning technique. This rough interface would result in unreliable data in the Auger scanning technique if one is not careful in selecting the scanning position in the specimen. Thus, for a more accurate determination of the concentration profile near the interface of the two materials, depth profile and line scanning technique should be employed at the same time.

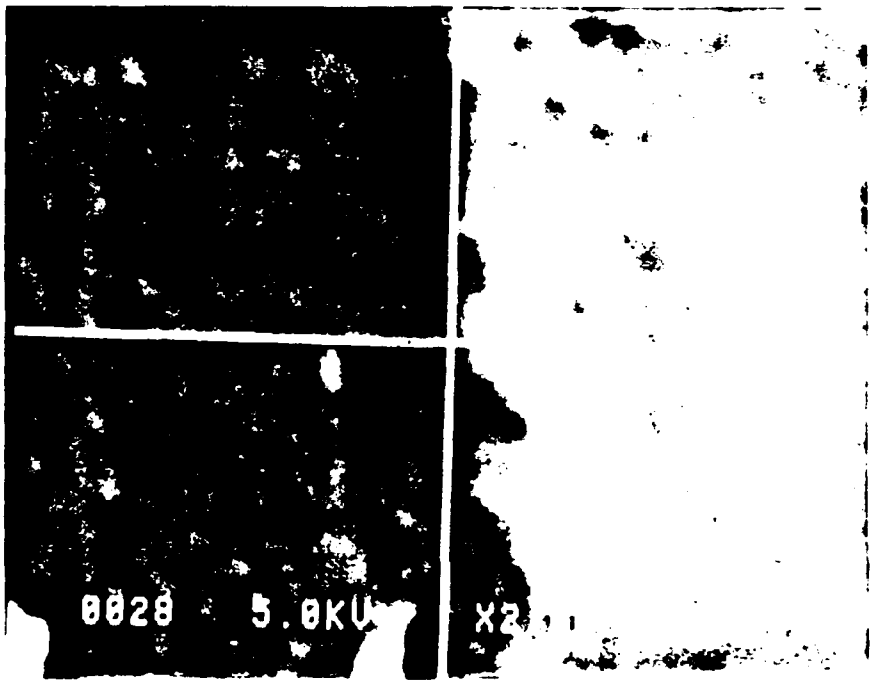

Figure 6. SEM picture of the angle-lapped surface of the SiC and AlN interface.

Zangvil and Ruh calculated approximate diffusion coefficients of SiC in AlN as 1×10^{-12} $cm^2 s^{-1}$ at 1950 ° C [4]. This value is very high compared to the diffusivities in Table I. There is about four orders of magnitude difference between them. It was suggested that the lattice diffusion of coupled Al-N and Si-C pairs was responsible for these high values. However, according to the data in the Table I, there are some differences in the diffusivity between Si and C or Al and N. These differences in the diffusivity suggest that the atoms diffuse individually at low temperatures although pair mechanisms may be operative at high temperature. As can be seen in the Table I, the diffusivity of each element varies depending on the position. This may indicate the necessity of the employment of the Boltzmann's method in the accurate determination of the diffusivity for the four elements. However, no distinct break of the concentration across the interface is observed for any of the four elements. It seems that the surface condition of the two materials is smooth and sufficiently clean for the atoms to cross the interface without additional difficulty. The higher diffusivity of carbon in AlN than in SiC

may indicate a grain boundary contribution in the AlN. These results confirm that the materials selection and the sample preparation procedure employed in this experiment are sufficiently good to provide reliable data.

E. Conclusions

1. The diffusivity of the four elements at the interface of the SiC-AlN at 1500° C is roughly calculated as 10^{-17} cm^2/s at 1500° C. This is about four orders of magnitude lower than the previous calculations at higher temperature.
2. No major problem has been found in the selection and in the sample preparation procedure employed in this experiment. However, for more accurate determination of the diffusivity with Auger spectroscopy, a wider raster is desirable in the depth concentration profile.

F. Future Plans

1. Determine the temperature dependence of the diffusivity via the use of diffusion anneals at 1500, 1550, 1600, 1650 and 1700° C will be tried.
2. At each of these temperatures, the anneals will be conducted for two different times, 50 hours and 200 hours for more accurate determination of the diffusivity.
3. To determine the existence of any new phases near the interface of the two materials, TEM will be employed.

G. References

1. W. F. Knippenberg et al., U.S. Patent No. 3,634,149, 1972.
2. N. D. Sorokin, Yu. M. Tairov, and V. F. Tsvetkov, "Study of the Composition of Solid Solution SiC-AlN and SiC-GaN by the Method of X-ray Spectral Analysis," p.227 in *Abstracts of Reports at the Third All-Union Symposium on Scanning Electron Microscopy and Analytic Methods for Studying Solids*, Zvenigorod. Nauka, Moscow, 1981.
3. Y. A. Vodakov, and E.N. Mokhov, "Diffusion and Solubility of Impurities in Silicon Carbide," pp. 508-19 in Silicon Carbide-1973, edited by R. C. Marshall, J. W. Faust, Jr., and C. E. Ryan, University Press, S. C., 1974.
4. A. Zangvil and R. Ruh, J. Mat. Sci. and Engr. **71** 159 (1985).

VI. Distribution List

	Number of Copies
Dr. Yoon Soo Park Office of Naval Research Applied Res. Division Code 1212 800 N. Quincy Street Arlington, VA 22217-5000	2
Administrative Contracting Officer Office of Naval Research Resident Representative The Ohio State University Research Center 1314 Kinnear Road Columbus, OH 43212-1194	2
Director Naval Research Laboratory ATTN: Code 2627 Washington, DC 20375	7
Defense Technical Information Center Bldg. 5, Cameron Station Alexandria, VA 22314	14